

Review Article

Open Access



Heterointerface engineering of polymer-based electromagnetic wave absorbing materials

Shan Liu¹, Dengfeng Zhou¹, Fang Huang¹, Min He^{2,*}, Shuhao Qin², Yongqian Shi^{3,*}, Pingan Song^{4,*} 

¹College of Materials and Energy Engineering, Guizhou Institute of Technology, Guiyang 550003, Guizhou, China.

²College of Materials and Metallurgy, Guizhou University, Guiyang 550025, Guizhou, China.

³College of Environment and Safety Engineering, Fuzhou University, Fuzhou 350116, Fujian, China.

⁴Centre for Future Materials, School of Agriculture and Environmental Science, University of Southern Queensland, Springfield, QLD 4350, Australia.

*Correspondence to: Prof. Min He, College of Materials and Metallurgy, Guizhou University, Jiaxiu South Road, Huaxi District, Guiyang 550025, Guizhou, China. E-mail: hemin851@163.com; Prof. Yongqian Shi, College of Environment and Safety Engineering, Fuzhou University, 2 Wulongjiang North Avenue, Fuzhou 350116, Fujian, China. E-mail: shiyg1986@fzu.edu.cn; Prof. Pingan Song, Centre for Future Materials, School of Agriculture and Environmental Science, University of Southern Queensland, 37 Sinnathamby Boulevard, Springfield, QLD 4350, Australia. E-mail: pingan.song@usq.edu.au

How to cite this article: Liu, S.; Zhou, D.; Huang, F.; He, M.; Qin, S.; Shi, Y.; Song, P. Heterointerface engineering of polymer-based electromagnetic wave absorbing materials. *Soft Sci.* 2025, 5, 7. <https://dx.doi.org/10.20517/ss.2024.69>

Received: 30 Nov 2024 **First Decision:** 2 Jan 2025 **Revised:** 9 Jan 2025 **Accepted:** 14 Jan 2025 **Published:** 18 Jan 2025

Academic Editor: YongAn Huang **Copy Editor:** Pei-Yun Wang **Production Editor:** Pei-Yun Wang

Abstract

Heterointerface engineering has drawn considerable interest in tuning interfacial polarization and promoting impedance matching. Therefore, it has become a key strategy for optimizing electromagnetic wave (EMW) absorption. This comprehensive review primarily focused on the EMW absorbing strategies of polymer-based materials, emphasizing the critical developments of heterointerface engineering. A possible EMW absorbing mechanism of polymer-based materials was proposed, emphasizing the synergism of multi-components, microstructure design, and heterointerface engineering. Key innovations in structural design such as porous structure, multilayered structure, and segregated structure are explored, highlighting their contributions to enhancing EMW absorption. Also, the review highlights the latest research progress of advanced conductive polymer-based and insulating polymer-based materials with desirable EMW absorption performance; their fabrication methods, structures, properties, and EMW absorption mechanisms were elucidated in detail. Key challenges on polymer-based EMW absorbing materials are presented followed by some future perspectives.

Keywords: Heterointerface engineering, electromagnetic wave absorption, polymer-based, structure design, multi-component



© The Author(s) 2025. **Open Access** This article is licensed under a Creative Commons Attribution 4.0 International License (<https://creativecommons.org/licenses/by/4.0/>), which permits unrestricted use, sharing, adaptation, distribution and reproduction in any medium or format, for any purpose, even commercially, as long as you give appropriate credit to the original author(s) and the source, provide a link to the Creative Commons license, and indicate if changes were made.



INTRODUCTION

With the booming growth of the electric industry and wireless communication, particularly the rapid development of 5G and various intelligent devices, high frequency in the gigahertz range has brought undesirable electromagnetic (EM) radiation pollution^[1-6]. It is another pollution that is challenging to manage after the water, noise, atmosphere, and solid waste^[7]. In the telecommunication, radar, military, aviation, and other scientific implementation areas, *etc.*, EM interference (EMI) can cause delicate electronic devices to malfunction, severely interfere with signal communication, and hinder the running of smart facilities and precision instruments, ultimately leading to system failure^[8-11]. Moreover, studies show that exposure to high electromagnetic wave (EMW) density poses risks to human health and increases the likelihood of diseases^[12-16].

To tackle the above-mentioned problems, the application of EMI shielding materials is an effective approach^[17-20]. The EMI shielding can be realized by reflecting or absorbing EMW. Secondary EM pollution could arise from the reflecting shielding materials. However, absorbent shielding materials are in high demand since they primarily absorb EMW and convert them into heat or other energy^[21-25]. The requirement for EMW absorbing materials that are suitable for usage environment and function is increasing. Generally speaking, the next generation of EM absorbing materials should have light weight, thin thickness, flexibility, strong absorption capability, outstanding impedance matching, and wide effective absorption bandwidth (EAB)^[22,26-29]. Nowadays, designing efficient EMW absorbers with multifunctionality is still quite challenging.

The major focus of the fabrication of EMW absorbers is metals, carbon materials, magnetic materials, conductive polymer materials, MXene, metal-organic frameworks (MOFs), and composite materials^[26,30-32]. Nonetheless, the traditional metal-based EMW absorbing materials have high density and are prone to corrosion. Carbon materials have low density and good electrical conductivity, but excellent absorbing materials also need good impedance matching performance. Therefore, carbon materials alone are not an ideal absorber and need to be improved^[30]. Because of their low density, remarkable resilience to corrosion, processability, moldability, high design flexibility, and tunable specific shielding capability, polymer-based materials hold great promise for the creation of advanced EMW absorbers^[1,33,34].

Generally, there are two strategies to improve microwave absorption. The first method is heterointerface engineering strategy which achieves an excellent impedance matching^[13]. Another method is to build absorbers with unique structures to increase their capacity to absorb EMW by regulating the surface and interface properties^[26,31,35-39].

EMW ABSORBING STRATEGY OF POLYMER-BASED MATERIALS

Absorption, reflection, and multi-reflections were the EMI shielding mechanisms. Materials with a reflection mechanism exhibit high electrical conductivity, where interactions between the EM field and charge carriers result in EMW reflections^[40]. The interactions of magnetic or electric dipoles produce the EMW absorption. The pores, interfaces, and flaws generated multi-reflections. In order to obtain appropriate EMW absorption properties, dielectric/magnetic loss, and impedance matching ought to be considered^[11,21,41].

The dielectric/magnetic loss and impedance matching of polymer-based EMW absorbers can be adjusted by cooperating conductive and dielectric components with magnetic material, adjusting the structure, and constructing heterointerfaces^[8,42-44]. **Figure 1** is the expected EMW absorbing mechanism of advanced polymer-based materials with multi-components, designed structures, and heterogeneous interfaces.

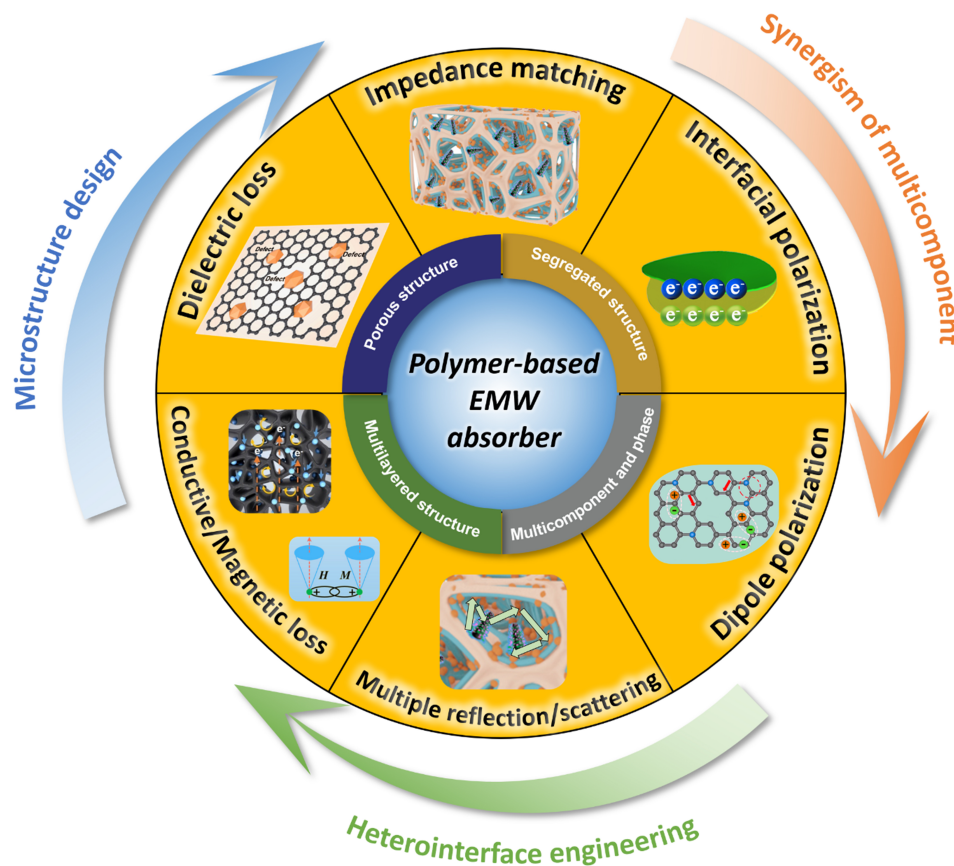


Figure 1. EMW absorbing strategy of advanced polymer-based materials combining heterointerface engineering, synergism of multi-components, and microstructure design. EMW: Electromagnetic wave.

HETEROINTERFACE ENGINEERING AND STRUCTURE DESIGN

A significant way to maximize the efficiency of magnetic absorbers is heterointerface engineering, which has drawn much attention to controlling the distribution of electrons at contacting interfaces^[37,45]. It is considered an advanced option to deal with complex EM environments and develop a new generation of smart EM materials. It is regarded as a cutting-edge solution to handle intricate EM situations and create a new class of intelligent EM materials.

The physicochemical reaction occurs when distinct interfaces are in contact, such as space charge orientation, energy band rearrangement, and electron migration. It impairs the loss of polarization and conductivity. Furthermore, the magneto crystalline anisotropy will be altered by the pinning effect and distortion defects, leading to magnetic loss including magnetic resonance, hysteresis loss, and eddy current^[46]. Crystalline/amorphous interfaces, crystallization/crystallization interfaces, and van der Waals heterostructures are examples of heterointerfaces. The heterointerface engineering strategy could integrate the unique functions of multi-components and phases, induce a remarkable interfacial polarization in the interface, and enhance impedance matching via rational assembly of material phases^[13]. For example, creating heterogeneous nanostructures into polymers is a promising method for designing efficient absorbers. The structures can improve EMW absorption using magnetic loss and dielectric polarization while maintaining a suitable impedance matching^[9].

The structure design is an appropriate way to enhance EMW absorption capabilities^[27]. It is based on the dispersive spatial distribution of nanoparticles, multiple scattering loss for the hierarchical structure, and interfacial polarization for large heterogeneous surfaces^[47]. Reasonable microstructures with multiple heterointerfaces can change the complex permittivity. In addition, the internal voids can generate multi-reflections and scatterings, enhancing the impedance matching and ability to attenuate EMW^[17]. Porous structures, multilayer structures, segregated structures, core-shell structures, hydrogel, aerogel, prefabricated conductive structures, *etc.*, were designed in conductive polymer composites (CPCs) to achieve high-efficiency microwave shielding^[48,49].

Multi-component composites

Because of their special characteristics and single loss mechanism, single-component systems can rarely achieve appropriate impedance matching and high absorption effectiveness^[7,50-53]. As a result, creating multi-component composites using materials such as carbon and conductive polymers can overcome the problem of high filling loading while also achieving synergistic effects between the components^[27,54].

By introducing a second or third component phase, EMW absorbing materials can provide sufficient heterointerfaces, abundant interfacial polarization, dielectric loss, and suitable impedance matching, thus enabling efficient EMW absorption^[55,56]. Owing to the variable charge distribution at the junction of two areas with different dielectric characteristics, the Maxwell-Wagner-Sillars effect is produced in a heterostructure. Meanwhile, a local dipole electric field will be formed by the capacitor-like interfaces; thus, the combined motions of interfacial dipoles enhance the response with EMW and EMW attenuation^[57-59].

Porous structure

Based on Maxwell-Garnett theory, internal multiple scattering, impedance matching, and the dielectric constant may all be enhanced by the porous structure with heterointerfaces^[29,57,60,61]. Specifically, because foaming concentrates conductive fillers in the cell walls and reduces the electrical threshold, porous CPCs need less filler to create conductive networks than compact CPCs^[10,34]. Meanwhile, the voids can produce a large number of solid/air interfaces and adjust the impedance matching. By enhancing interfacial polarization, reducing conductivity close to the polymer-gas interfaces, and prolonging the shielding/absorption propagation path, these interfaces offer extra EMW shielding/absorption capabilities^[9,62]. Therefore, balancing conduction loss, polarization loss, impedance matching, and attenuation capability is a potential advancement in heterogeneous porous CPCs^[29,37,63].

In-situ polymerization, phase inversion, supercritical CO₂ foaming, freeze drying, 3D printing, and thermally induced phase separation are some methods that can be successfully used to create porous polymer-based EMW absorption materials^[34].

Multilayered structure

The multifunctional demands are rarely met by CPCs with homogenous structures. For example, to satisfy the requirements of infrared stealth and Joule heating, anisotropic thermal conductivity (TC) and electrical conductivity are required. By creating continuous conductive networks and increasing multi-scattering, a 3D multilayered structure may increase EM absorption and realize infrared stealth by preventing heat transfer^[7,9,64]. Constructing a multilayered structure is a promising method to realize anisotropy. Fully utilizing the advantages of single components to achieve the applicability of multiple functions is a perfect approach to achieving anisotropy^[15].

The layered structure includes randomly multilayered structures, gradient distribution structures, sandwich-like structures, alternating multilayered structures, and “brick and mortar” structures, *etc.*^[65]. By varying the EM characteristics and thickness of each layer in the multilayer absorber, frequency-tunable EM absorption performance and wide EAB can be achieved^[20,66]. Usually, an EM reflection layer, an EM adsorption interlayer, and a surface impedance matching layer contribute to a multilayered structure. Although some EMW may enter the EMI adsorption material from the surface impedance matching layer, the EM loss occurs only in the interlayer^[67]. In addition, the development of multilayered structures improved the interfacial polarization by creating a special multi-reflection/multi-absorption mechanism^[24,57,65].

Segregated structure

CPCs with conventional structures, in which the conductive fillers are randomly distributed, used for EM absorption often require a high conductive filler loading to meet the required EMI shielding effectiveness (EMI SE). However, extensive conductive fillers not only increase the fabricating cost but also reduce the mechanical properties of the CPCs^[68]. It has been proven that the creation of separated structure is a successful approach to realize high EM absorption at low filler loading^[69,70].

In the segregated structure, because of the volume exclusion effect of polymer microcells, the conductive network was condensed to a dense state, where conductive fillers are enriched in the interface or one polymer phase^[18]. This would lower the percolation threshold, improve the EMI SE of the material, and help create optimized conductive pathways at low filler loadings^[68,69,71]. In addition, the electron leaping, interfacial polarization, and interfacial reflection/scattering for EMW could all increase with the development of multiple interfaces in EMW shielding materials. Therefore, by regulating the arrangement of conductive fillers and creating multi-interfaces, the segregated structure is a successful strategy to fulfill the EMI shielding^[48].

RESEARCH PROGRESS OF POLYMER-BASED EMW ABSORBERS

Conductive polymer-based EMW absorbers

Conductive polymers are made up of repeating structural units joined by single and double bonds to produce conjugate bonds. Electrical conductivity benefits from their unique π -conjugated structure. Conductive polymers have been regarded as promising EM absorbing materials in past decades because of their lightweight, ease of synthesis, good stability and conductivity^[27,55,72]. The composites based on intrinsically conductive polymers, including polypyrrole (PPy) and polyaniline (PANI), offer advantages in terms of ease of processing, corrosion resistance, high electrical and TC, good dielectric properties^[18,40,73]. They can easily achieve impedance matching and optimized conductivity by adjusting their EM characteristics^[48,72,74].

Conductive polymers are dielectric loss materials that release EM energy through micro- or macro-current and polarization loss. However, relying solely on dielectric loss rarely satisfies the requirements for EMW absorption. Therefore, combining several loss mechanisms is often used for constructing high-performance EMW absorbers^[75-77].

PANI

PANI has low density, low cost, simple synthesis, tunable conductivity, good thermal stability, reversible redox reaction, ease of doping, nontoxicity, and environmental stability^[73,78]. It can be coupled to other materials through *in-situ* polymerization to create composites with core-shell structures that construct rich heterogeneous interfaces^[29] and improve the conductance loss and impedance matching^[55,79]. Intrinsic PANI

exhibits high permittivity, often acting as a dielectric component to synthesize multi-component EMW absorbing composites^[3,80].

For example, MXene/PANI composites were fabricated via electrostatic self-assembly. The PANI bridged the MXene to construct a 3D structure that prolongs the EMW transmission path, and balanced the impedance matching of MXene. The dipole and interfacial polarization provided efficient EMW attenuation. When the thickness of the composite was 2.3 mm, the EAB reached 8.64 GHz, while the composite containing 10 wt% PANI had a reflection loss (RL) of -60.6 dB and an EAB of 6.0 GHz^[55]. In another study, a PANI-modified Co/N-doped C (Co-NC@PANI) with a sea urchin-like structure was prepared, and then it was incorporated into an MXene-based gel by freeze-drying. The Co-NC@PANI tuned the dielectric constant of MXene, introduced a magnetic loss, and optimized interfacial polarization and impedance matching. The gelatin optimized the conductive transmission path [Figure 2A]. The RL and EAB of the aerogel at 1.8 mm reached -62.4 dB and 6.56 GHz, respectively^[31]. An Au@MXene/cellulose nanocrystal/dodecylbenzenesulfonic acid doped PANI (AMCP) film was fabricated via vacuum-assisted filtration. Due to the heterointerface engineering, the film had an EMI SE of 67.9 dB. It achieved 100 °C in 5 min by an infrared lamp, and maintained stable photothermal conversion. It was also endowed with thermal stealth capability due to the gaps between the layers [Figure 2B]^[73].

A Fe₃O₄/PANI composite was fabricated by hydrothermal reaction and chemical oxidative polymerization. The hollow Fe₃O₄ and PANI enhance the interfacial polarization, multi-reflection and scattering loss [Figure 3A]. The composite at 1.84 mm with a heterogeneous interface had a minimal RL (RLmin) of -55.03 dB and a maximum EAB (EABmax) of 4.88 GHz. An EAB of 5.16 GHz (12.84-18 GHz) and an RL of -40.47 dB were achieved at 1.88 mm^[75]. A PANI@FeSiAl composite was fabricated as an EMW absorber by *in situ* oxidative polymerization. The heterogeneous interface between FeSiAl and PANI provided conductive and polarization loss by charge orientation, interfacial polarization, and defects in the PANI layer [Figure 3B]. The composite at 1 mm had an RLmin of -37.87 dB^[78]. A core-shell hydroxylated boron nitride (BN-OH)@Fe₃O₄@PANI nanocomposite was fabricated as an EMW absorber by *in-situ* growth. The Fe₃O₄ and conductive PANI resulted in magnetic and electrical loss, and the EMW had multi-reflection in the composite [Figure 3C]. The RLmin reached -49.85 dB at 11.36 GHz, and the EAB reached 8 GHz (8.5-16.5 GHz) at 3 mm. The TC of the composite with dopamine and hydroxyl as interfacial modifiers was 0.98 W·m⁻¹·K⁻¹^[35]. PANI/La-doped BaFe₁₂O₁₉ (PANI/La-BaM) composite was developed. With 10% of La concentration, the RL and EAB of the composite reached -47.83 dB and 3.98 GHz. This was attributed to conductivity loss and dipole polarization from PANI, eddy current from La-BaM, multi-reflection and scattering, and interfacial polarization^[80]. A MoS₂/Fe₃O₄/PANI nanocomposite was fabricated. The composite had optimized impedance matching and multi-interfacial polarization; the RLmin reached 50.3 dB at 2.6 mm and the EAB reached 5.1 GHz. The EMW absorption was realized in the whole X and Ku-band^[76].

A PANI/sludge fly ash material was fabricated via interfacial polymerization. The composite at 2.82 mm had an RL of -54.11 dB at 10.00 GHz with an EAB of 4.08 GHz. It was ascribed to the combined effect of magnetic and dielectric loss^[79]. Acrylonitrile-methylmethacrylate copolymer C microsphere was modified with capsaicin-like 3,5-dimethylphenol derivative (DMPD) to fabricate a dielectric EM absorption material. Functional groups of C-O, -C-N, -NO and dipole polarization were introduced by DMPD. The heterointerfaces increased the interface polarization. The RLmin of -63.10 and EABmax of 6.81 GHz (8.95-15.76 GHz) were achieved at 2.5 mm^[81]. PANI/biomass-derived porous C (BPC) composites were prepared. The PANI prompts heterogeneous interface and interfacial polarization loss. It also acted as a bridge on BPC to form conductive networks, which improved multi-reflections and scattering, and conduction loss.

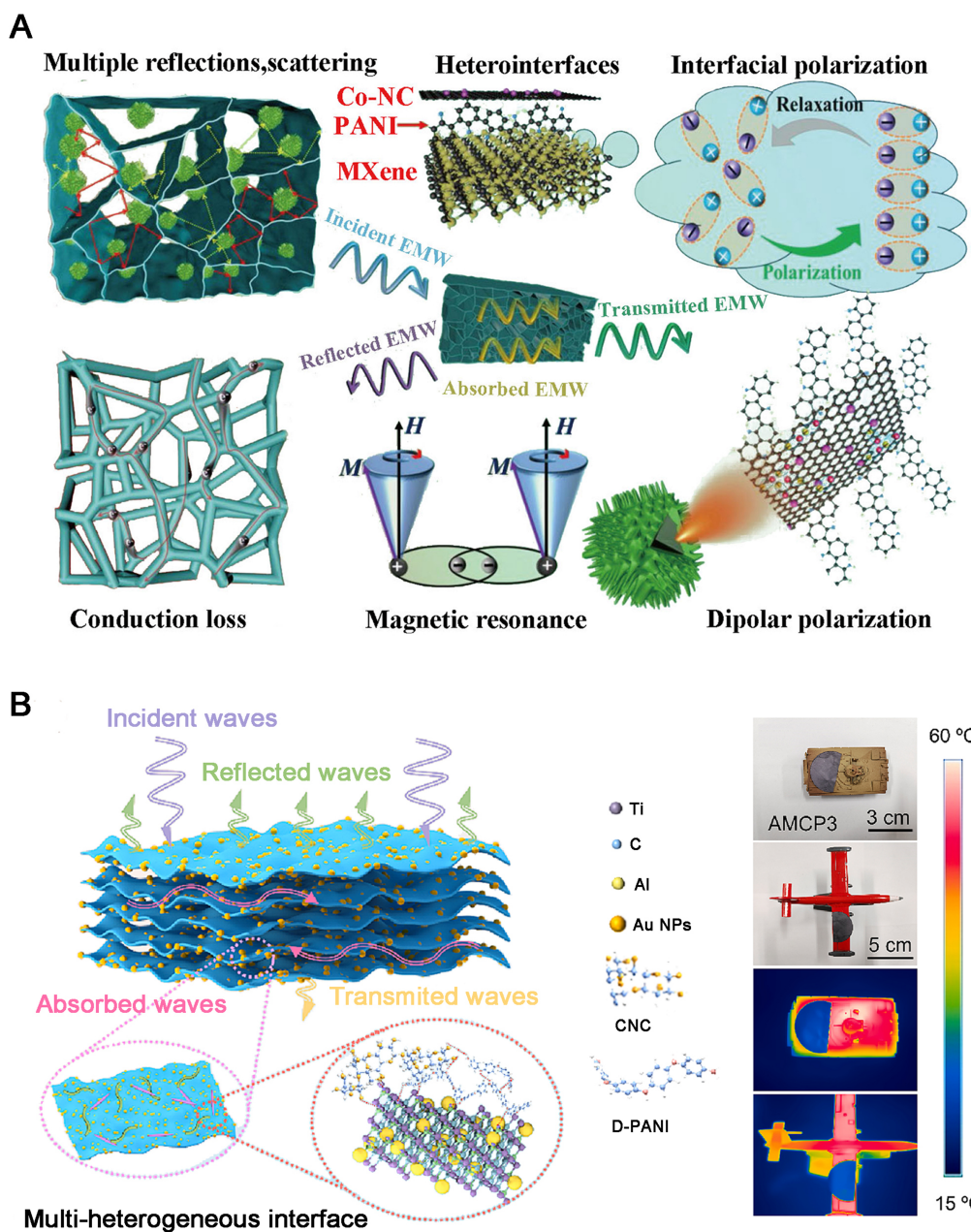


Figure 2. The EMW attenuation mechanism and other functions of PANI/MXene-based materials. (A) The illustration of the EMW absorption mechanism of Co-NC@PANI^[31]; (B) Schematic diagram of EMW attenuation of AMCP film. Infrared thermograms of model and overlay models of AMCP film^[73]. EMW: Electromagnetic wave; PANI: polyaniline; AMCP: Au@MXene/cellulose nanocrystal/dodecylbenzenesulfonic acid doped PANI.

The balances of polarization and conduction, attenuation capability, and impedance matching were achieved. The composite had an RL_{min} of -40.89 dB at 2.6 mm and an EAB of 4.24 GHz at 2.1 mm^[29]. In another study, a PANI/graphene oxide (GO) layer was attached to bamboo powder (BP) through interfacial polymerization. The impedance matching of the PANI was achieved with the corporation of GO. The capability of dielectric storage and loss was enhanced. BP served as a cavity for reflection, which brings EMW loss channels and multi-reflections. The composite at 3 mm had an RL_{min} of -44 dB at 9.36 GHz, and had an EAB of up to 5.36 GHz within the 12.64-18 GHz range at a thickness of 2 mm^[82].

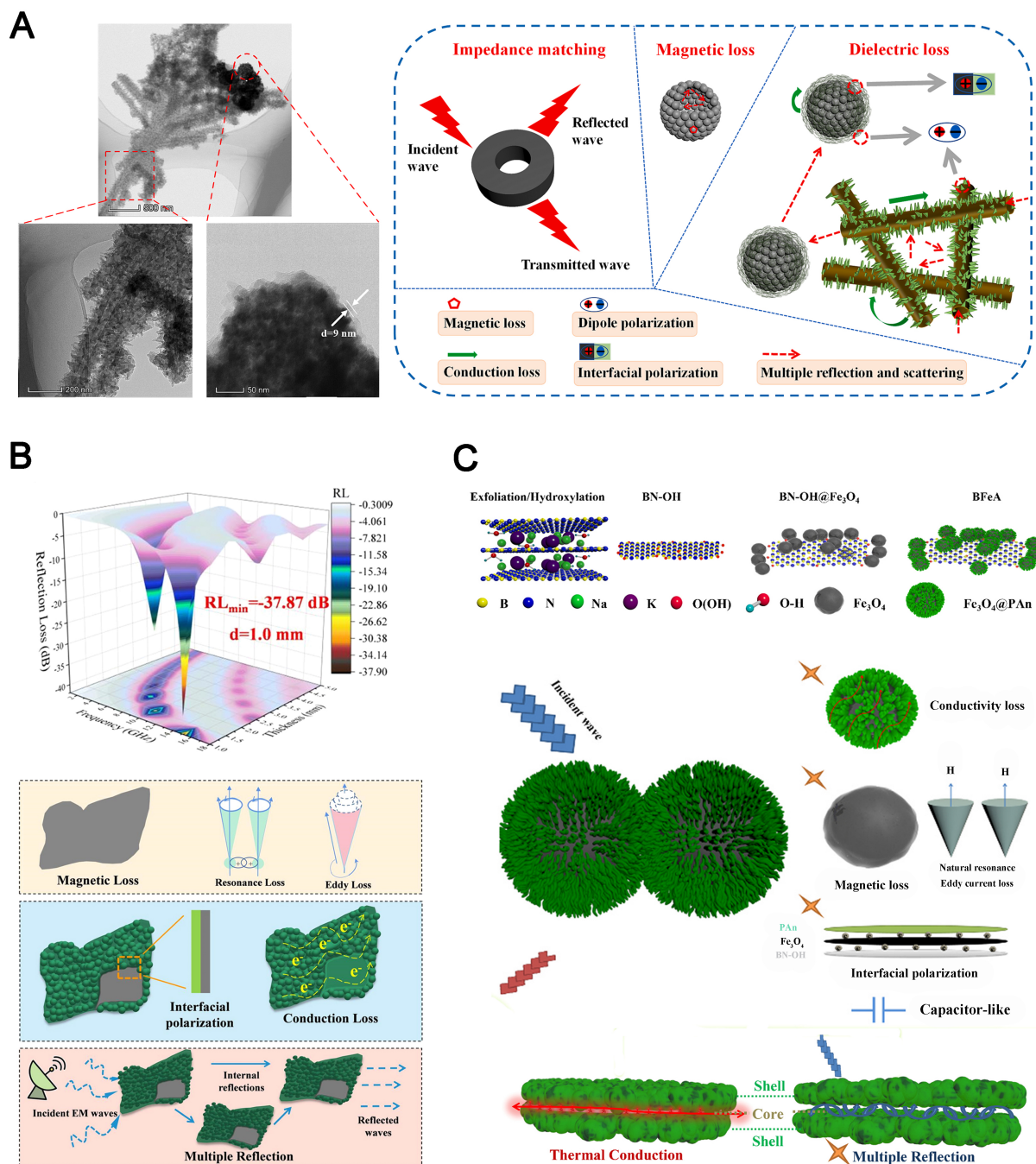


Figure 3. The morphology, EMW absorption mechanism, and property of Fe-doped PANI composites. (A) A TEM image, partial enlarged views, schematic diagram of EMW absorption mechanism of $\text{Fe}_3\text{O}_4/\text{PANI}$ composite^[75]; (B) 3D plots of RL, the EMW absorption mechanism of PANI@FeSiAl composites^[76]; (C) Schematic diagram of EMW absorption and thermal conduction of BN-OH@ Fe_3O_4 @PANI composite^[35]. EMW: Electromagnetic wave; PANI: polyaniline; TEM: transmission electron microscopy; RL: reflection loss; BN-OH: boron nitride.

PPy

PPy is a significant conductive polymer with convenient preparation, tunable conductivity, chemical stability, and resistance to corrosion^[11,47]. Its high electrical conductivity makes it highly capable of absorbing EMW. The conductivity may be adjusted by varying the permittivity through changes in the filler and

polymerization degree^[44]. It can further increase its EMW absorption capability by efficiently increasing the interfacial polarization and conduction loss^[63]. Because of the impedance matching and heterostructures of Fe₃O₄@PPy (FP), the composite at 2.08 mm had an EABmax of 6.00 GHz (12.0-18.0 GHz). Heterostructure provided the polarization fields and conduction and magnetic loss, and the PPy shell afforded dielectric loss^[47].

The hydrothermal reaction, *in situ* polymerization, freeze-drying, and reduction were used to prepare a FP microsphere decorated reduced GO (rGO) [Figure 4A]. FP consumed EMW by dielectric and magnetic losses. rGO functioned as a multi-reflection layer and formed conductive networks. FP and rGO improved the impedance matching. The composite achieved an EAB of 5.26 GHz at 1.71 mm and an RLmin of -61.20 dB at 1.89 mm^[44]. C-coated FeCoNi (FeCoNi@C) spatially confined within hollow carbon nanoboxes (HCNB) were prepared using core-shell FeCoNi Prussian blue analogs (PBAs)@PPy as precursors. Because of the differences in thermal stability of PPy and FeCoNi PBAs, the derivative had a yolk-shell structure if the inward contraction of the core caused by heat was greater than the interface contact; otherwise, it had a hollow structure. The yolk-shell sample had an EABmax of 5.8 GHz and an RLmin of -52.4 dB, which results from the synergism of dielectric and magnetic losses, and the superior impedance matching [Figure 4B]^[23]. ZnFe₂O₄@PPy microspheres were prepared using pyrolysis and *in situ* polymerization [Figure 4C]. The core-shell structure of ZnFe₂O₄@PPy optimized the impedance matching, with an RLmin of -41 dB and an EBA of 4.1 GHz. The polarization from the heterointerfaces by the wrinkle structure, combined with the conductivity of PPy leading to conduction loss, jointly contributed to the increased dielectric loss^[8]. NiFe₂O₄/PPy composites with negative permittivity were prepared by surface-initiated polymerization. The RLmin of -40.8 dB was observed in the composite with 40.0 wt% of NiFe₂O₄/PPy at 1.9 mm. The EAB reached 6.08 at 2.08 GHz, which was attributed to improved impedance matching and the synergism of conduction loss, magnetic loss and dielectric loss^[11].

A PPy/CaCu₃Ti₄O₁₂/CoFe₂O₄ was prepared via *in-situ* chemical oxidative polymerization. A bowl-like structure was formed because of the interfacial interactions of PPy and nanofillers. The periphery of the cup consisted of CaCu₃Ti₄O₁₂ and CoFe₂O₄. The composite had an EMI SE of 30 dB, with the combined magnetic and dielectric losses, losses from free charges in the interface, interfacial polarization, and the wedge effect responsible for the absorption-dominated mechanism [Figure 5A]^[40]. A PPy@Co/CoFe₂O₄@hollow bowl-like C (PPy@Co/CoFe₂O₄@HNBC) was prepared. PPy and Co/CoFe₂O₄ were added via *in-situ* growth and polymerization after HNBC was created using a template approach. The composite at 1.90 mm had an RLmin of -61.85 dB at 12.80 GHz and an EAB of 5.60 GHz at 1.70 mm, which was attributed to its distinct structure and the combined effects of natural and exchange resonance-induced magnetic loss, conduction and polarization-induced dielectric loss [Figure 5B]^[63].

A conductive MOF Cu₃(HHTP)₂ (hexahydroxytriphenylene, HHTP) was packed on the PPy by hydrothermal polymerization. MOFs improved interfacial polarization, conductive loss and impedance matching, which benefited EM absorption. The EAB of the material can reach 6.68 GHz (11.00-17.68 GHz). The RLmin and EAB of the composite at 2.7 mm reached -59.34 dB and 6.42 GHz^[13]. MXene was loaded with co-substituted beta(2)-Keggin-type polyoxometalate doped PPy and Fe₃O₄. As a proton acid doped PPy, polyoxometalate and HCl could adjust the impedance matching and conductivity. Fe₃O₄ caused multiple polarization and magnetic loss; dipoles, defects, and dangling bonds caused dipole polarization; and the charge accumulated at the interface caused interfacial polarization. The composite at 1.7 mm with 45 wt% filling had an RLmin and EAB of -62.6 dB and 9 GHz^[72].

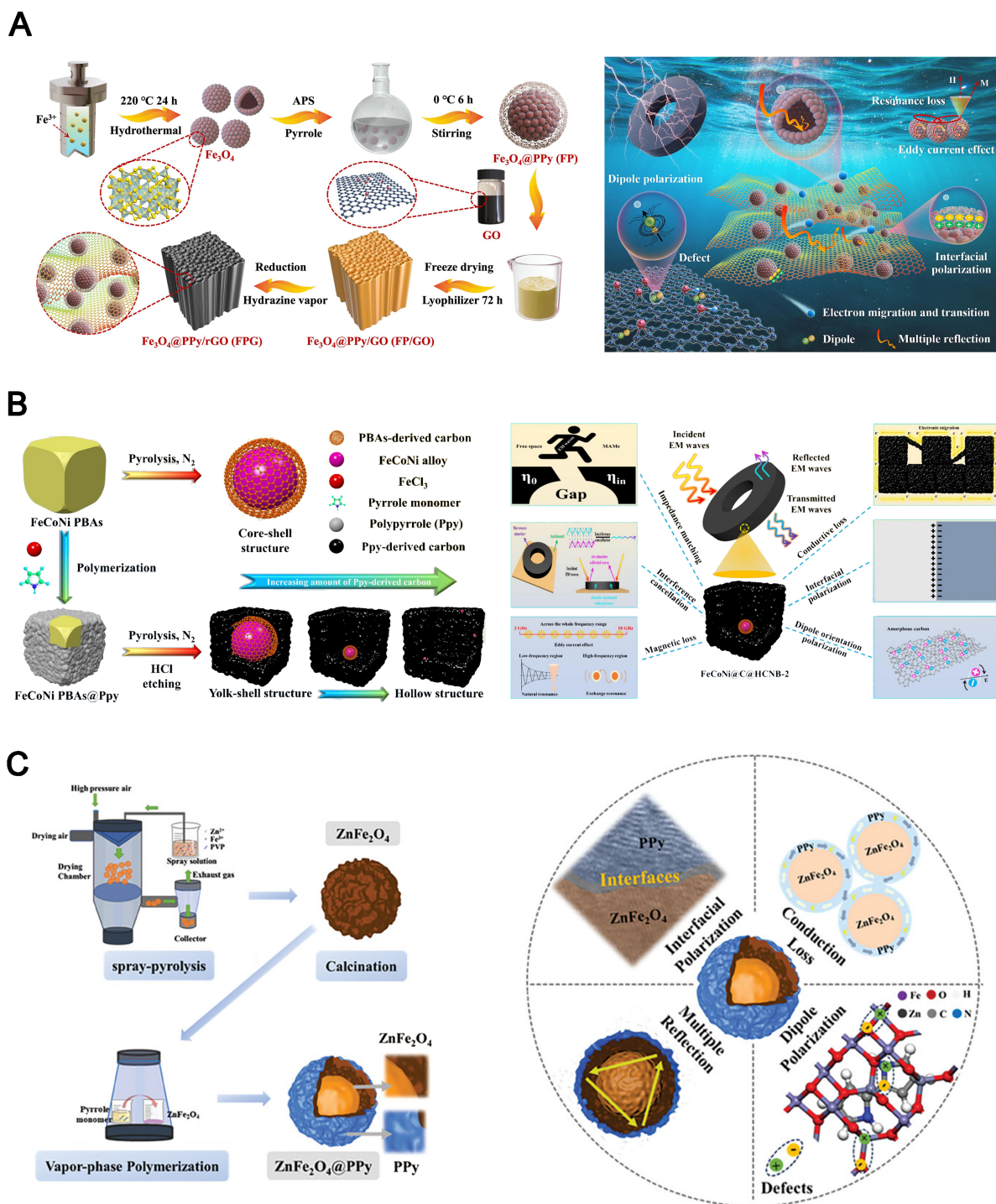


Figure 4. The fabrication methods and EMW absorption mechanisms of (A) Fe_3O_4 @PPy/rGO^[44]; (B) FeCoNi @PPy derived C@HCNB ^[23]; (C) ZnFe_2O_4 @PPy^[8]. EMW: Electromagnetic wave; PPy: polypyrrole; rGO: reduced graphene oxide; HCNB: hollow carbon nanoboxes.

Polythiophene and its derivatives

Polythiophene (PTH) and its derivatives are a typical class of conductive polymers. For instance, poly(3,4-ethylenedioxythiophene) (PEDOT) has strong electrical conductivity and is a promising candidate in EM

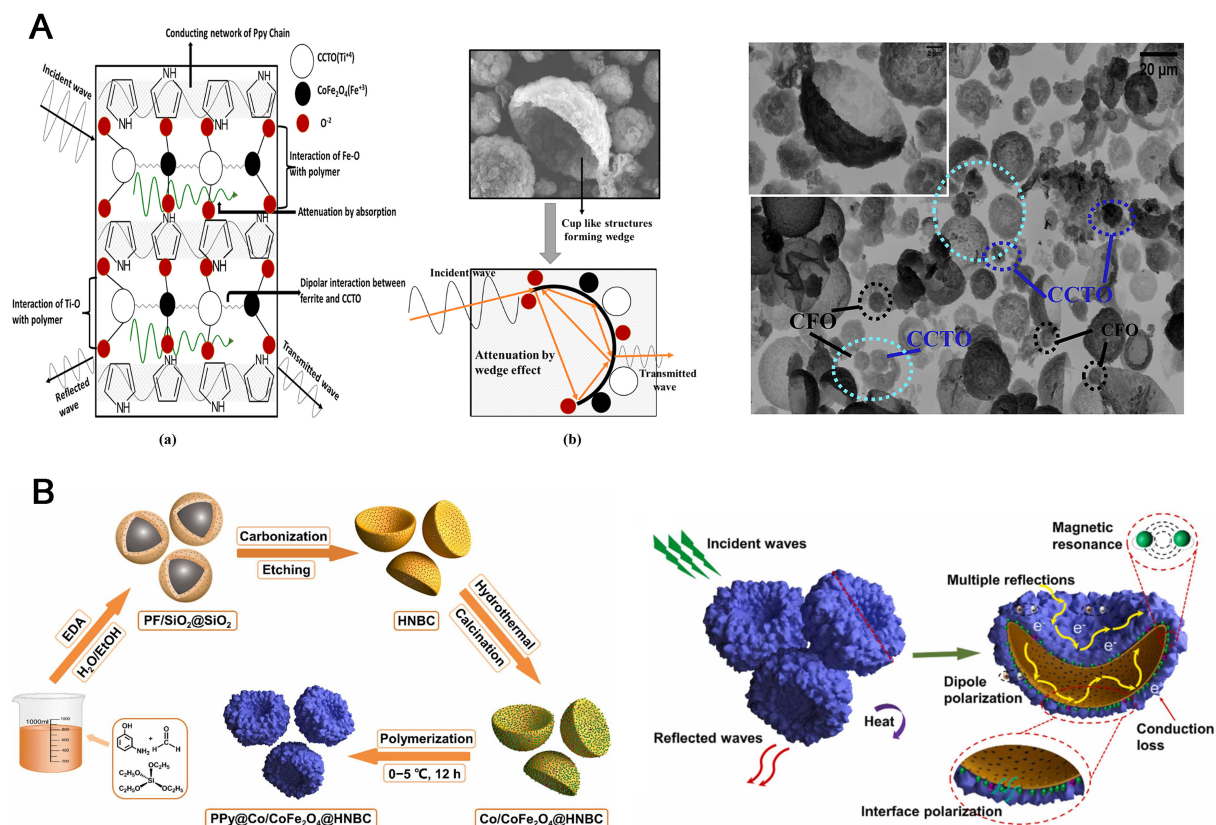


Figure 5. The morphology, fabrication method, and EMW absorption mechanism of CoFe₂O₄/PPy-based composites with bowl-like structure. (A) The morphology and EMW absorption mechanism of PPy/CaCu₃Ti₄O₁₂/CoFe₂O₄ composite^[40]; (B) The fabrication method and EM absorption mechanism of PPy@Co/CoFe₂O₄@HNBC^[63]. EMW: Electromagnetic wave; PPy: polypyrrole; EM: electromagnetic; HNBC: hollow bowl-like C.

absorption because the PEDOT contains conjugated π electrons^[7]. PEDOT was used with other magnetic or dielectric materials to improve interfacial polarization and dielectric loss, which improves impedance matching and EM adsorption^[83].

A CoSe₂@PTh with a core-shell structure was prepared by hydrothermal treatment and *in-situ* polymerization. The conductive network from PTh, heterointerfaces from the core-shell construction, and optimized impedance matching by multi-component all contribute to enhanced EM absorption performance [Figure 6A]. The composite at 1.76 mm had an RL_{min} of -55.40 dB and an EAB of 5.8 GHz. A MoS₂@PEDOT/rGO composite was prepared by oxidative polymerization and microwave thermal reduction. By introducing PEDOT, the defects in GO were repaired *in situ*, regulating the conductivity and polarization of the composite [Figure 6B]. Benefiting from improved conductivity, interfacial and dipole polarization, and superior impedance matching with the addition of PEDOT/rGO, the RL_{min} and EAB of the composite reached -32.41 dB at 2.1 mm, and 7.04 GHz under 20 wt% filler loading^[7]. Ti₃C₂T_x MXene/PEDOT:poly(styrenesulfonate) (PSS) and aramid nanofiber (ANF) were combined to prepare a double-layer film. The interface between MXene and ANF was enhanced by PEDOT:PSS. The composite film with a conductive layer of 4.4 μ m had an EMI SE of 48.1 dB, a mechanical strength of 155.9 MPa, and a toughness of 19.4 MJ·m⁻³. When the film was 47 μ m, the EMI SE rose to 63.7 dB. Moreover, the film had a photothermal conversion of 59.6 °C at 100 mW⁻² and Joule heating ability of 382 °C at 4 V^[22]. N-doped carbon nanofibers (NCNFs) were coated with PEDOT to form composite fibers. When 10 wt% of paraffin

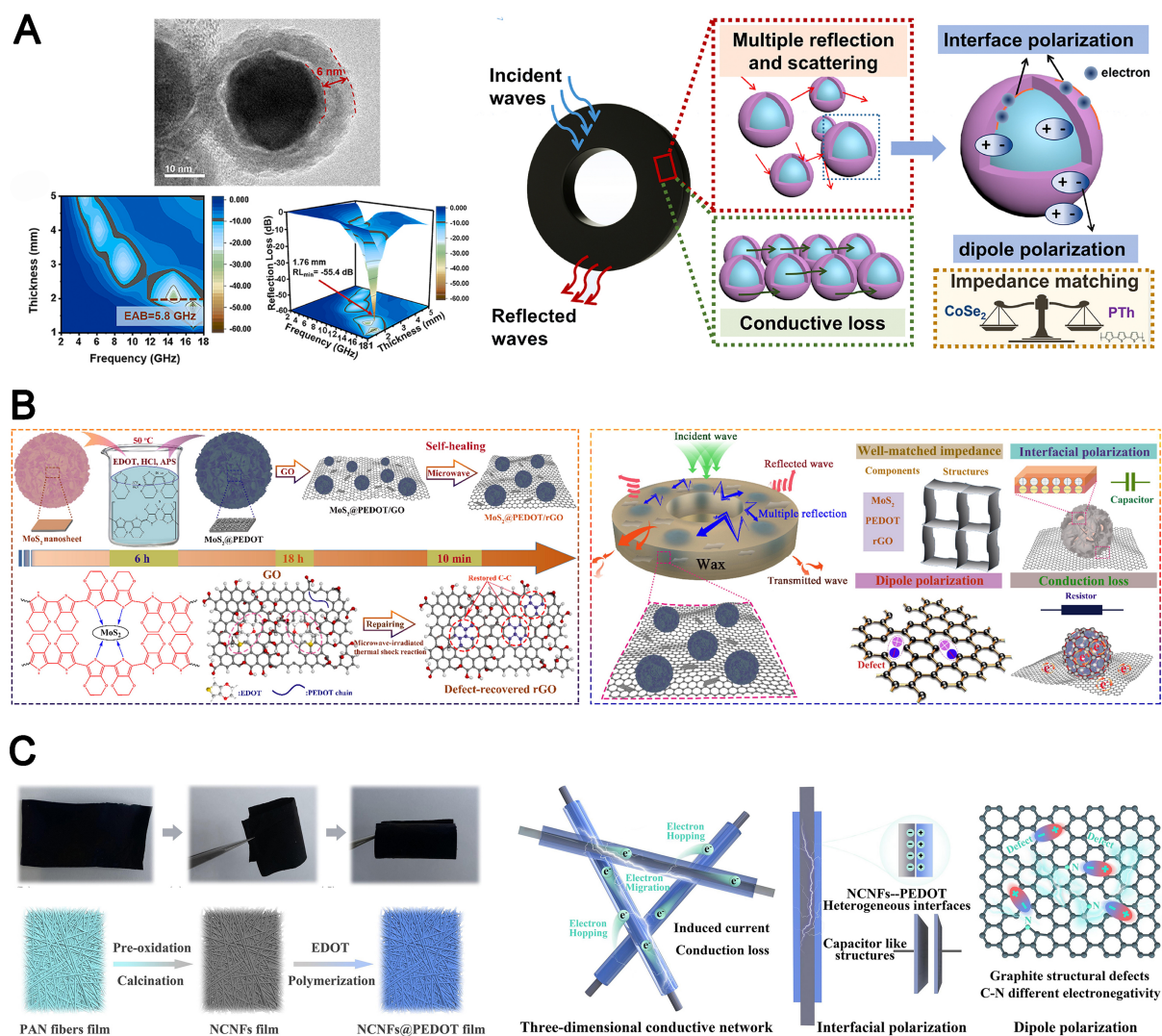


Figure 6. The morphology, fabrication method and EMW absorption mechanism of PTh-based materials. (A) Morphology, 3D plots of RL and EMW absorption mechanism of CoSe₂@PTh^[27]; (B) The fabrication and EMW absorption mechanism of MoS₂@PEDOT/rGO^[71]; (C) The fabrication, bending and rolling states, and EMW absorption mechanism of NCNFs/PEDOT^[83]. EMW: Electromagnetic wave; PTh: polythiophene; RL: reflection loss; PEDOT: poly(3,4-ethylenedioxythiophene); rGO: reduced graphene oxide.

was added to the composite with dual 3D conductive networks, the RL reached -66.9 dB at 2.6 mm. The EAB reached 6.72 GHz (9.6-16.32 GHz) at 2.7 mm with 5 wt% of filler, which was ascribed to the interfacial polarization between NCNFs and PEDOT, the conduction loss, and dipole polarization result from N doping and defects in graphite [Figure 6C]^[83].

PDA

Polydopamine (PDA) often acts as a component to synthesize multi-component EMW absorbing composites. Its functional groups such as -NH₂ and catechol facilitate the formation of the inorganic-organic core/shell structure with desired electron-hole separation efficiency^[84,85]. Moreover, the PDA with N-doped graphene structure has electrical conductivity, and the pyrolyzed PDA has excellent conductivity similar to N-doped GO. Thus, it is anticipated that the pyrolyzed PDA will balance the mechanical and electrical performances of composites with a broad EAB^[86].

CoNi-MOFs-derived CoNi was anchored onto core-shell Ni@C. By cooperating with PDA, the interface of CoNi-MOFs and NiO was enhanced by electrostatic interaction. Because of the multiple conductive networks, magnetic interaction, and interfacial polarization, the composite had good microwave absorption. The RL_{min} reached -51.4 dB at 1.9 mm, and the EAB was 4.6 GHz at 1.3 mm^[26]. The zeolitic imidazolate framework (ZIF)-derived C was introduced into carbonyl iron (Fe/FeCo@C) via *in situ* dopamine polymerization on the carbonyl iron and pyrolysis. The multiple polarization effect from heterogeneous interfaces increased the EMW absorption. The conductive network combined magnetic and dielectric loss to optimize impedance matching. A Fe/FeCo@C/PP composite was prepared by fused deposition modeling. The composite with 40% filling had an RL_{min} reached -60 dB at 1.7 mm, and an EAB of 4.75 GHz at 1.5 mm^[21]. PDA-derived C@MXene composite was fabricated via *in-situ* polymerization and pyrolysis. The composite at 2.8 mm with 7.5 wt% filling had an RL_{min} of -46.92 dB and an EAB_{max} of 7.01 GHz. The combination of MXene and PDA created defects that caused dipole polarization, triggered heterogeneous space charge and electron density distribution to increase interfacial polarization and provided excellent impedance matching^[46]. Salt template impregnation was used to prepare a composite foam with resorcinol terephthalaldehyde resin and a porous pyrolyzed PDA/carbon nanotube (CNT)-Fe₃O₄. The conductivity and mechanical characteristics of the foam improved by 168% and 74 times, respectively, because of the pi-pi interactions and conductivity of the filler. Due to conductivity loss and interfacial polarization, the EAB was 8.32 GHz and the RL_{min} was -33.0 dB^[86].

Insulating polymer-based EMW absorbers

Recently, polymer-based composite materials consisting of insulating polymers and electrically/thermally conductive fillers have received considerable attention in EMW shielding and absorption due to their lightweight, abundant varieties, flexibility, easy processing, low cost, resistance to corrosion, excellent shielding performance, and tunable electrical properties^[10,87]. To enhance the EMI shielding, the conductive fillers are joined to one another to create a conductive channel. To further enhance EMI shielding and absorption, conductive fillers can be used as dielectric and magnetic loss materials^[88,89].

The insulating polymer matrix for EMW absorption can be both thermosets such as polydimethylsiloxane (PDMS), epoxy resins (EP) or polyurethanes (PU) and thermoplastics such as poly(vinylidene fluoride) (PVDF) or cellulose nanofibrils (CNFs)^[90-92].

PDMS

A sandwich structure with a MXene@SiO₂ interlayer was prepared via solvent induced phase separation method, and then compounded with PDMS. The composite had large specific surface area of 545.42 m²·g⁻¹. The MXene@SiO₂ increased the packing density and sedimentary mode of the filler, and enhanced the EMI SE to 43.3 dB, mechanical strength of 4.61 MPa^[24]. A composite made of layers of metalized polyimide (PI), Fe₃O₄@PDMS dipped melamine-formaldehyde (MF), and Ni-coated melamine foam was prepared via layer-by-layer stacking. The multilayer structure enhanced the interface polarization loss and expanded the propagation pathway. An EMI SE of 54.20 dB was obtained because of the interfacial polarization loss and EM loss caused by Fe₃O₄ and Ni. The foam also had flame retardancy with a limiting oxygen index (LOI) of 27%^[93]. A poly (l-lactide) (PLLA)/PDMS/multi-walled CNT (MWCNT) composite with honeycomb-like conductive networks was fabricated using PLLA as a volume-occupying phase. The EMI SE of the composites with etched 300 μm spherical micro-particles with rough surfaces achieved 35.1 dB, with absorption dominated mechanism^[68]. Aligned NCNF/barium titanate (CNF-BaTiO₃)/PDMS composite was prepared by electrospinning and carbonization. The composite at 0.24 mm with the aligned fillers had an EMI SE of 81 dB, while the EMI SE of non-aligned composite was 59.2 dB. The alignment increased interfacial polarization, internal reflections, electrical conductivity, and electronic conduction in axial direction of the fiber^[28]. PDMS microcells and the continuous PDMS/CNT were chemically bonded to

prepare a segregated structure in PDMS/CNT composite. The EMI SE of the composite with 2.2 vol% of CNT was 47.0 dB. In contrast to the traditional segregated composite, the tensile strength and elongation at break of the obtained composite were 3.6 MPa and 87.0%, respectively, increasing by 35.0 and 7.0 times. After 1,000 stretching-releasing at a strain of 30%, the EMI SE retention was 80%^[69]. In another study, segregated SiO₂ particles were added to the PDMS/MWCNT composite to provide numerous interfaces and a volume exclusion effect. The composite containing 3.0 vol% MWCNT and 32.4 vol% SiO₂ had an EMI SE of 61.4 dB^[48].

EP

Silicon carbide nanoparticles were fabricated by carbothermal reduction, and were added into EP to form a composite. The RL_{min} and EAB of the composite at 4.25 mm with 20 wt% of SiC is -62.02 dB and 7.7 GHz. The composite at 4.50 mm had an EAB_{max} of 8.1 GHz, shielding nearly the whole X-band and Ku-band. The interfacial enhanced the EMW absorption. Under microwave radiation, the shape memory recovery took 31 s, and the deformation efficiency and shape recovery rate rose by 125.81% and 17.84% compared with pure EP^[19]. A Fe₃O₄@SiO₂/MXene interlayer structure was fabricated by electrostatic self-assembly. The Fe₃O₄@SiO₂ increased the interlayer spacing of MXene and elongated the propagation path. The heterostructure achieved high impedance matching because of the combination of magnetic and dielectric effect, and prolonged MW propagation pathway. The hetero-interfaces boost polarization and dielectric loss. The RL_{min} of the Fe₃O₄@SiO₂/MXene/EP composite at 1 mm reached -60.9 dB^[94]. An EP/melamine-derived carbon foams@LDH composite was prepared by *in situ* growth and vacuum deposition. The porous structure and the heterointerface prolonged the EM transmission path and provided abundant interfaces and polarization sites; the composite with 10 wt% filler loading exhibited an RL_{min} of -57.77 dB and an EAB of 7.20 GHz (from 10.48 to 17.68 GHz). Moreover, it had high TC (0.62 W·m⁻¹·K⁻¹) and flame-retardancy performance^[95]. EP composite was prepared by the synergy of CNT/AgBNs on long-range CF felt skeletons. The CNT/AgBNs improved the interfacial bonding between EP and CF, and alleviated the phonon scattering at the interface. The TC of the composite was enhanced by 333% compared to EP. The composite had an EMI SE of 51.36 dB because of the multiple reflection and adsorption promoted by the multiple heterointerfaces^[96].

PU

A thermoplastic PU (TPU)/graphene composite foam was prepared by phase separation method. Due to the dipole polarization, conduction loss, interfacial polarization loss and multi-scattering, the foam at 3.1 mm with 3 wt% graphene had an RL_{min} of -51.86 dB and an EAB of 4.28 dB (12.6-17.0 GHz). Due to improved impedance matching, the composite with the same amount of Fe₃O₄ as graphene had an RL_{min} of -58.96 dB^[87]. A MoS₂/rGO/TPU foam was fabricated by vapor-induced phase separation. The MoS₂/rGO prevented rGO restacking and reinforced the TPU. The EMI SE of the foam at 3 mm with 7 wt% MoS₂/rGO was -32 dB due to electric dipoles, and carrier hopping resulted from multi-reflections and heterointerfaces^[34]. A TPU/CoFe₂O₄/graphite composite was prepared. Because of interfacial and dipole polarization, synergistic dielectric and magnetic loss, conduction loss, and multiple scattering, the composite at 5 mm with 15 wt% CoFe₂O₄ and 35 wt% graphite showed an EMI SE of 41.5 dB in 8.2-12.4 GHz^[97].

A PU composite elastomer assisted by coral reef-like MXene/CNT@Fe₃O₄ was prepared. Due to the synergism of magnetic, conduction, and polarization loss, the composite at 4 mm had an RL_{min} of -54.81 dB. It showed a good sensitivity for strain sensing and human motion monitoring. Its thermal diffusion capability was 155.9% higher than that of pure PU, and it remained stable at 200 °C^[98]. A film was fabricated consisting of a top layer of PU/Fe₃O₄NPs and a bottom layer of Ag nanoparticles (AgNPs)/PU by

interfacial fusing utilizing photothermal treatment. The EMI SE of the film reached 69.6 dB. It also had high mechanical performance, photothermal and electrothermal conversion ability and stability^[99]. Blast furnace slag was introduced into phenolic resin and then prepared a C-slag composite by PU template technique and carbonization. Due to interfacial polarization, dielectric and magnetic losses, the foam at 2 mm with 20% slag had an EMI SE of 48.9 dB with 40 dB absorption, thermal insulation and stability up to 500 °C^[41]. A FeSiAl@acrylic PU (PUA)@SiO₂ composite was prepared. The SiO₂ and PUA were introduced by sol-gel, *in-situ* polymerization, and plasma-enhanced chemical vapor deposition. The PUA/SiO₂ improved impedance matching and interface polarization, decreased the dielectric constant. The RL_{min} of the composite at 2.3 mm reached -47 dB, while the EAB reached 5.3 GHz, covering almost the entire Ku-band. The corrosion resistance was also increased^[43].

PVDF

Multi-layered rGO-Co₂Z hexaferrite-PVDF nanocomposite film was prepared by the solution casting method. rGO-Co₂Z hexaferrite improved interfacial polarization through charge accumulation at the interfaces. The maximum magnetization of the film was 8.9 emu/g at 300 K. Due to the combination of magnetization and electrical polarization [Figure 7A], the EM SE of the film at 0.861 mm was 54.09 dB^[2]. Coaxial wet-spinning assembly was used to prepare core-shell fibers with PVDF shell and MXene core. The PVDF hydroxylation enhanced the interfacial interaction [Figure 7B]. The electrical conductivity and an elongation at break of the fiber was $3.08 \times 10^5 \text{ S}\cdot\text{m}^{-1}$ and 16%. The PVDF shell prevented erosion and oxidation of the MXene core. A MXene/PVDF textile with a 6 μm MXene layer exhibited an EMI SE of 60 dB and a Joule heating performance^[100]. A PVDF/MXene aerogel with anisotropic structure was prepared by directional freezing and freeze-drying. The aerogel had highly aligned MXene due to the hydrogen bonding and van der Waals interactions between MXene and PVDF. As a result of the increased conduction loss and multi-reflections [Figure 7C], the EMI SE of the aerogel in the transverse direction and freezing direction were 53 and 45 dB dominated by the absorption^[101].

A layered GNP-PVDF/MXene composite film was fabricated using a blade-coating method. The film developed a well-contacted in-plane conduction network, with a high electrical conductivity of 7,423 S/m, an in-plane TC of $36.9 \text{ W}\cdot\text{m}^{-1}\cdot\text{K}^{-1}$, an EMI SE of 36.3 dB. Moreover, the film reduced the light-emitting diode (LED) heating temperature by more than 15 °C^[88]. A CNT-graphene-NiCo chains/PVDF film was fabricated by solution mixing and compression. The EMI SE and electrical conductivity of the film were 63.3 dB and 9.12 S/cm, which was ascribed to the electrical conductivity of CNT-graphene-NiCo, dielectric and magnetic loss, interfacial polarization, and multi-reflections^[90]. The CNT/PVDF foam functioned as a shielding layer, while MXene@SiCnw heterostructure was added into the PVDF foam as an absorption layer. The two layers can adjust the electrical conductivity and impedance. The film had an EAB of 5.54 GHz and an EMI SE of 45 dB, nearly covering the whole Ku-band^[9].

ANFs and CNFs

Polymer-based nanofiber materials have become attractive options for EMI shielding and adsorption. They are usually used to build 3D aerogel and obtain carbon aerogel by carbonization. For example, it is possible to use CNFs with high mechanical performance as the matrix and connecting bridge of fillers, to create a porous structure and enhance the dispersion of fillers^[14]. Enhanced EMI SE results from their large surface-to-volume ratio, which makes it easier to have absorption sites^[102]. The combination of porosity and electric/magnetic coupling loss can alleviate the impedance mismatching, which allows EMW to enter aerogels rather than being reflected right away^[103].

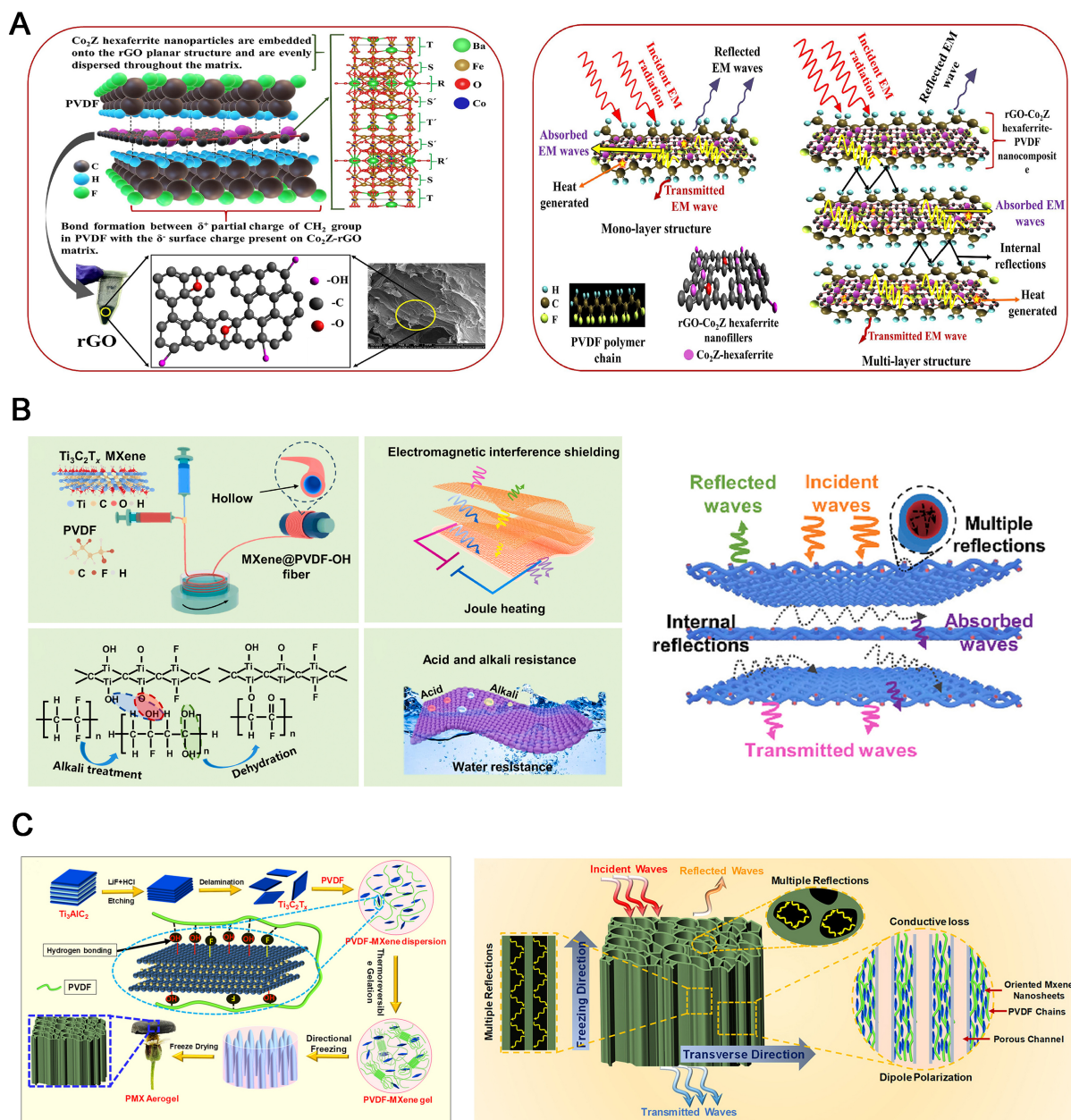


Figure 7. The structure, fabrication method and EM absorption mechanism of PVDF-based materials. (A) The structure and EM absorption mechanism of rGO-Co₂Z hexaferrite-PVDF^[2]; (B) The structure and EM absorption mechanism of MXene/PVDF textile^[100]; (C) The fabrication and EM absorption mechanism of PVDF/MXene aerogel^[101]. EM: Electromagnetic; PVDF: poly(vinylidene fluoride); rGO: reduced graphene oxide.

For example, CoNi-MOFs, ANFs, and CNFs were combined to form a CoNi@C/ANF/CNF carbon aerogel (CoNi@C/ACA) by freeze-drying and carbonization [Figure 8A]. Due to the multiple reflections of heterointerfaces, dipolar/interfacial polarizations, and magnetic/dielectric losses, the aerogel with 1.8 wt% loading had an RL_{min} of -66.57 dB and an EAB of 6.3 GHz. It also had Joule heating properties and thermal stability. The aerogel reached 75 °C in 15 s at 6 V and kept stable for 600 min^[14]. Directional freezing and freeze-drying were used to create a Ti₃C₂T_x/ANF aerogel based on the van der Waals forces and hydrogen bonds. The aerogel had high elasticity and a compressive strength of 93.59 kPa. The sites of impedance

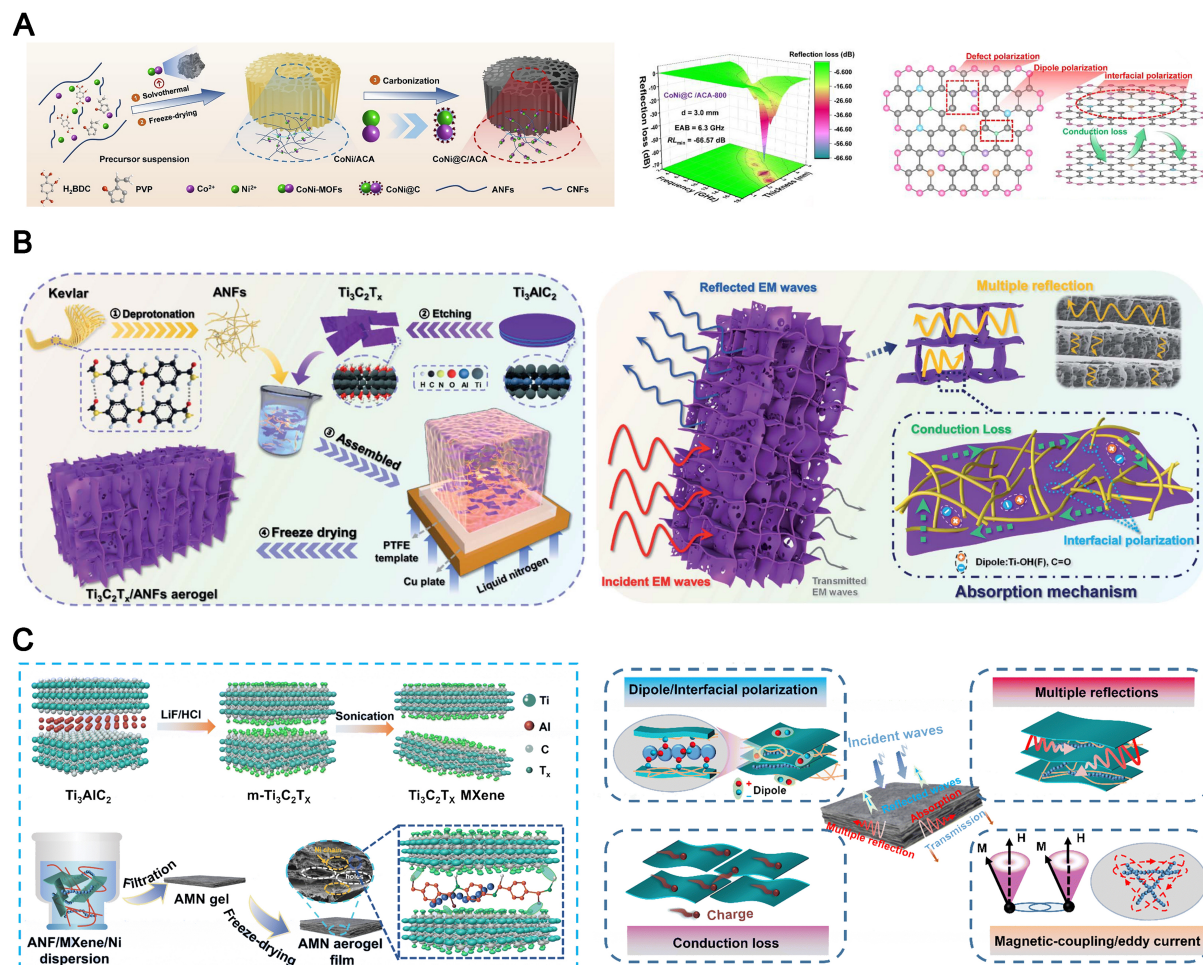


Figure 8. The fabrication method and EM absorption mechanism of ANF-based aerogels. (A) The fabrication, 3D plots of RL and EM absorption mechanism of CoNi@carbon/ANF/CNF carbon composite^[14]; (B) The fabrication and EM absorption mechanism of Ti₃C₂T_x/ANF aerogel^[104]; (C) The fabrication and EM absorption mechanism of ANF/MXene/Ni film^[50]. EM: Electromagnetic; ANF: aramid nanofiber; RL: reflection loss; CNF: cellulose nanofibril.

mismatch and conductive loss increased as a result of the Ti₃C₂T_x forming conductive channels. The interfacial polarization was introduced by the cell wall structure [Figure 8B]. The conductivity, EMI SE, and specific shielding effectiveness (SSE)/t of the aerogel with 0.58 vol% of filler reached 854.9 S·m⁻¹, 65.5 dB, and 11,391 dB·cm²·g⁻¹. The EMI SE maintained 59.1 dB after at 250 °C for 2 h^[104]. ANF/MXene/Ni aerogel was prepared via filtration and freeze-drying. Due to the porous laminar structure and the magnetic/electric synergistic network with various conductive paths [Figure 8C], the tensile strength, RL_{min}, and EAB of the aerogel were 30 MPa, -48.6 dB at 1.5 mm, and 5.8 GHz, respectively, almost covering the entire Ku band^[50].

A chitosan-derived C/rGO/CNTs/Co/SnS₂/SnS aerogel was prepared via bidirectional freeze-drying, chemical bath deposition and carbonization. The multilayer C extended the transmission path and accelerated the electron migrating; SnS and SnS₂ induced heterointerfaces, S vacancies and C defects; the internal electric field was formed, resulting in polarization and conductivity loss. The aerogel had an EAB of 8.4 GHz at 2.4 mm and an RL_{min} of -56.1 dB at 2.7 mm. The aerogel also achieved visible light and infrared stealth ability^[64]. A CNT@ZnIn₂S₄ nanosheets/CNF aerogel (CNTs@ZIS/CNF) was fabricated. The aerogel had an EM absorbing property with an EAB of 5.8 GHz at 2.7 mm. It was ascribed to improved polarization

loss from interfacial coupling effects and superior impedance matching from multilayered porous materials [Figure 9A]. It also had a secondary recovery, multi-absorption, and heat-insulating abilities^[105]. ZIF-67/MXene/CNF carbon aerogel was fabricated by freeze-drying and carbonization. The porous structure and the synergy of magnetic/electric loss facilitated the impedance matching. Heterointerfaces induced interfacial and dipole polarization [Figure 9B]. The aerogel had an EMI SE of 86.7 dB and an absorption coefficient of 0.72^[103]. Vacuum-assisted filtration was used to prepare a six-layered film with alternating CoFe₂O₄@MXene/CNF layers and AgNWs/CNF layers. Due to the magnetic/electric coupling, multi-scattering and absorption [Figure 9C], the film at 0.1 mm had an EMI SE of 87.8 dB with a reflection of 5.6 dB. After being attacked chemically and physically, it retained 97% of its EMI SE. It also had a tensile strength of 183.2 MPa, an in-plane TC of 6.875 W/(m center dot K) and a Joule heating performance of over 90 °C at 3.0 V in 20 s. The inferior through-plane TC provided an infrared stealth performance^[15]. Cotton-derived flexible carbon fiber (CF)/rGO was prepared by electrostatic self-assembly, and then NiCo-layered double hydroxides (LDH) were arranged on CF/rGO to form a core-sheath structure composite. The composite at 2.5 mm had an RL of -60.9 dB at 10.3 GHz and an EBA of 6.1 GHz with 20 wt% filling. The carbonized CF contains heteroatoms, enhancing the dielectric loss caused by polarization. rGO facilitated the conductive loss. The voids created by the stacked LDH induced the reflection and scattering of EMW and optimized the impedance [Figure 9D]^[106].

PI

PI has thermal stability and high mechanical properties, multi-reflection and scattering, and EM absorption can be facilitated by PI composite foam. A strategy to increase the EM attenuation of composite foam is to add conductive and/or magnetic fillers to create a conductive network inside PI foams, as pure PI displays weak EM absorption due to its intrinsic low dielectric constant^[1,107].

A MXene@PI foam was prepared by directional freezing, freeze-drying, thermal imidization, and dip-coating. The cation- π interaction enhanced the PI framework and the interfacial interaction. The structure of the foam was tubular in the vertical freezing direction and honeycomb-like in the parallel freezing direction. With the same MXene loading, the EMI SE of the foam was 62.7 dB in the vertical direction, 158.0% greater than that in the parallel direction, and 109.7% greater than that of the isotropic foam^[1]. A Ti₃C₂T_x MXene/PI nanofibrous aerogel was fabricated via freeze-drying and thermal imidization. The porous 3D network improved multi-reflections and scattering and offered good matched impedance. The heterostructure enhanced the interfacial polarization, whereas the functional groups and defects on MXene caused dipole polarization. The aerogel exhibited an RLmin of -37.9 dB and an EAB of 3.3 GHz. It also had a low TC of 35.2 W·m⁻¹·K⁻¹ and high compression properties^[107].

Polysiloxane and its derivatives

A multilayered composite was prepared using liquid polycarbosiloxane-derived SiOC, ZrO₂/SiO₂, and nano ZrB₂ by hot press curing and pyrolysis. The composite showed an EAB of 4.2 GHz at 2.9 mm and an RLmin of -59.34 dB because of the excellent impedance matching and EMW loss caused by the conductive loss and multilayer interfacial polarization. It also had thermal insulation, oxidation resistance, and a notable decrease in radar cross-section^[67]. A Co-SiCN ceramic was prepared by the mixing of polysilazane and ZIF-67 and then pyrolysis. To optimize their impedance matching, the ZIF-67 encouraged the production of dielectric loss phases, such as CoSi, SiC, and free C. An EAB of 3.0 GHz at 1.05 mm and an RLmin of -46.4 dB at 6 GHz were attained due to the impedance matching and heterointerface polarization^[108]. A silicon oxycarbonitride (SiOCN) ceramic bowl was prepared from a hollow polysilsesquioxane by pyrolysis. Multi-reflections/scattering and impedance matching were enhanced by the bowl structure. Dipolar and interfacial polarization sites were generated by the hetero-nanodomains between the SiOCN and free C phase. The ceramic bowl exhibited an RLmin of -52.93 dB at 2.3 mm and an EAB of 3.88 GHz at 1.6 mm^[109].

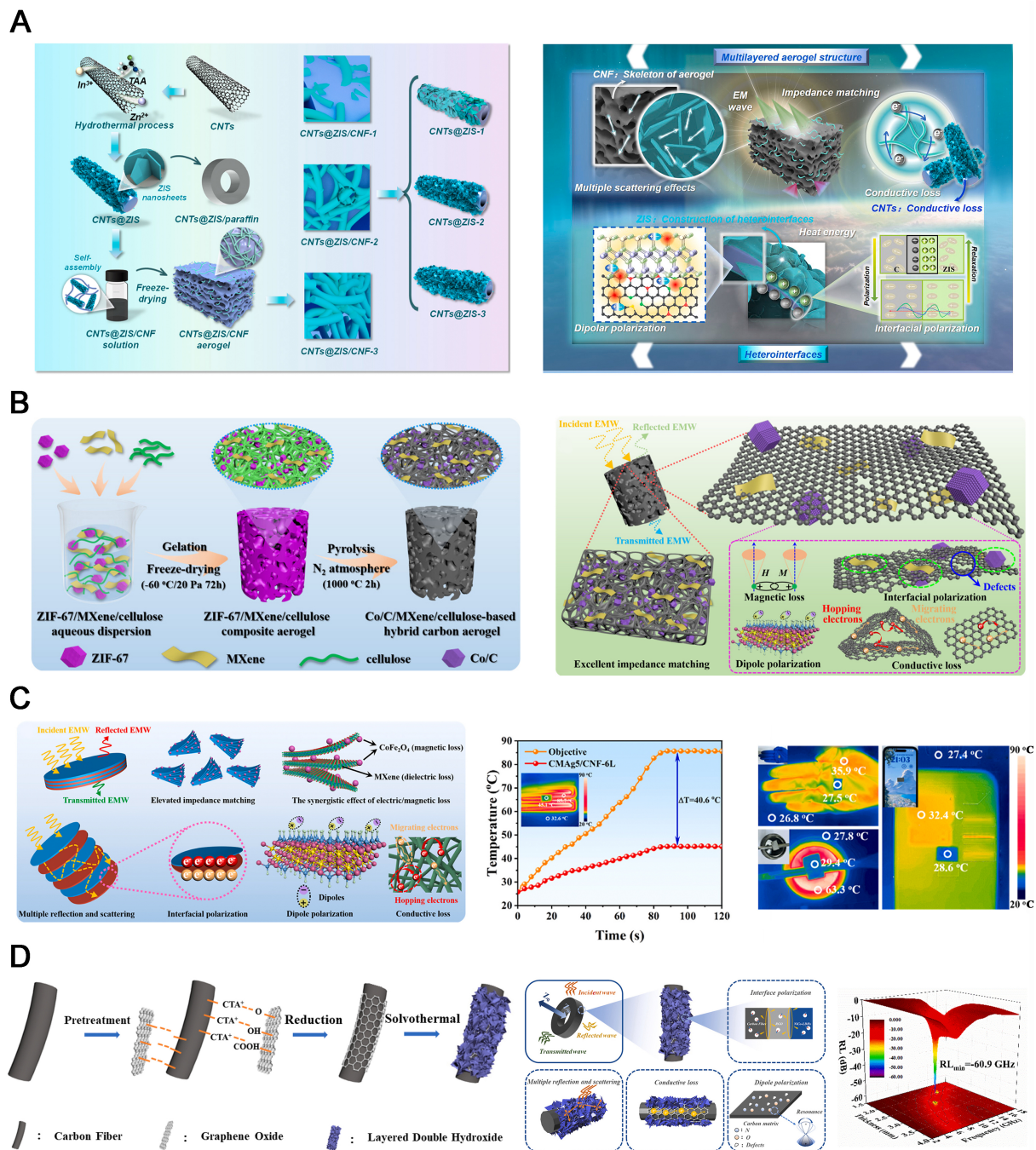


Figure 9. The fabrication method and EM absorption mechanism of CNF-based materials. (A) The fabrication and EM absorption mechanism of CNTs@ZIS/CNF aerogel^[105]; (B) The fabrication and EM absorption mechanism of ZIF-67/MXene/CNF carbon aerogel^[103]; (C) The EM absorption mechanism, Joule heating and infrared stealth performances of CoFe₂O₄@MXene/CNF-AgNWs/CNF film^[15]; (D) The fabrication, EM absorption mechanism and 3D plots of RL of CNTs@ZIS/CNF aerogel^[106]. EM: Electromagnetic; CNF: cellulose nanofibril; CNTs: carbon nanotubes; ZIF: zeolitic imidazolate framework; RL: reflection loss.

In summary, polymer-based EMW absorbing materials offer advantages due to their lightweight, flexibility, easy processing, low cost, and resistance to corrosion. They can easily achieve impedance matching and optimized conductivity. Intrinsically conductive polymers have good dielectric properties, often acting as a dielectric component to synthesize multi-component EMW absorbing composites. They can release EM energy by current and polarization loss. In order to construct high-performance EMW absorbers, conductive polymers cooperate with other materials to obtain several loss mechanisms. Insulating polymers are often used to combine with electrically conductive fillers to obtain excellent shielding performance and tunable electrical properties. The conductive fillers are joined to one another to create a conductive channel. To further enhance EMI shielding and absorption, the conductive fillers can serve as either dielectric or magnetic loss materials. Composites based on thermoplastics have good plasticity and processability in the preparation of EMW absorbing materials. However, their poor thermal resistance limits their application in high temperatures and long-term exposure to EM. Composites based on thermosetting plastics are brittle and cannot be molded repeatedly, but they have strong heat resistance, high hardness and strength, and often have good stability and durability when used as EMW absorbing materials.

CONCLUSION AND OUTLOOK

Advanced polymer-based EMW absorbers that can satisfy the requirements of high-absorbing ability, tunable EM properties, strong RL, wide EAB, low filler loading, thin thickness, and lightweight have become a research hotspot. To achieve these goals, the magnetic/dielectric loss and impedance matching of polymer-based EM absorption materials can be maximized by cooperating with multi-components, adjusting the structure, and introducing heterogeneous engineering.

Heterointerface engineering strategy introduces various defects including heteroatom doping, vacancies, dislocations, and twinning. The interfacial polarization generated by the heterointerfaces optimizes the impedance matching and dielectric loss. The structure design strategy determines the intrinsic loss capacities, conductive networks and conductive loss, and interfacial effects of polymer-based absorbers. Many absorbers based on conductive polymers (such as PANI and PPy) and insulating polymers (such as PDMS, EP, PU, and PVDF) have achieved desirable EMW absorption performance through a combination of multi-components, structural design and heterointerface engineering strategies.

However, emerging cutting-edge industries and the military have raised higher requirements for EMW absorbing materials. Developing polymer-based EMW absorption composites with increased matrix area and the contacting area between multi-components, thus obtaining larger heterogeneous interfaces, is a worthwhile research topic. Moreover, it is necessary to have a clear understanding of controlling of conductive phase structure, size, shape, even distribution and the interaction of multi-phase interfaces. The effects of porosity on the conductivity, the dielectric permittivity and EMW absorption need further study. The methods for optimizing the microstructure and geometric shape of each layer of polymer-based EMW absorption materials also need to be studied in detail. Therefore, a more comprehensive strategy combining theoretical computations and experimental research is required to gain deeper insights into the relationships between the structure and properties of polymer-based EMW.

In addition, the development of polymer-based EMW absorption materials with multifunctionalities such as heat conductivity, fire retardancy, joule heating or photothermal properties has practical significance. Furthermore, there is a need to develop multispectral stealth materials capable of simultaneously addressing microwave, infrared, and visible bands.

DECLARATIONS

Authors' contributions

Project administration, conceptualization, investigation, writing - review and editing: He, M., Qin, S., Song, P.

Investigation, writing - review and editing: Zhou, D., Huang, F., Shi, Y.

Writing - original draft: Liu, S.

Availability of data and materials

Not applicable.

Financial support and sponsorship

The authors acknowledge financial support from the National Natural Science Foundation of China (Grant No. 52163011), the Youth Talent Program of Guizhou Education Department (Qianjiaoji[2024]338), and the Science and Technology Project of Guizhou Province (QianKeHe ZhiCheng[2023] General 146; QianKeHe Pingtai Rencai CXTD[2023]012).

Conflicts of interest

All authors declared that there are no conflicts of interest.

Ethical approval and consent to participate

Not applicable.

Consent for publication

Not applicable.

Copyright

© The Author(s) 2025.

REFERENCES

1. Zhuo, L.; Shen, D.; Gou, P.; et al. Anisotropic high-strength polyimide-based electromagnetic interference shielding foam based on cation- π interaction. *Chem. Eng. J.* **2023**, *477*, 146992. DOI
2. Chakraborty, T.; Saha, S.; Gupta, K.; et al. An effective microwave absorber using multi-layer design of carbon allotrope based Co₂Z hexaferrite-polymer nanocomposite film for EMI shielding applications. *Chem. Eng. J.* **2024**, *487*, 150323. DOI
3. Palsaniya, S.; Mukherji, S. Enhanced dielectric and electrostatic energy density of electronic conductive organic-metal oxide frameworks at ultra-high frequency. *Carbon* **2022**, *196*, 749-62. DOI
4. Liu, S.; Chevali, V. S.; Xu, Z.; Hui, D.; Wang, H. A review of extending performance of epoxy resins using carbon nanomaterials. *Compos. Part. B. Eng.* **2018**, *136*, 197-214. DOI
5. Yan, Y.; Zhang, K.; Qin, G.; et al. Phase engineering on MoS₂ to realize dielectric gene engineering for enhancing microwave absorbing performance. *Adv. Funct. Mater.* **2024**, *34*, 2316338. DOI
6. Gao, Z.; Iqbal, A.; Hassan, T.; Hui, S.; Wu, H.; Koo, C. M. Tailoring built-in electric field in a self-assembled zeolitic imidazolate framework/MXene nanocomposites for microwave absorption. *Adv. Mater.* **2024**, *36*, e2311411. DOI
7. Zhang, S.; Pei, Y.; Zhao, Z.; Guan, C.; Wu, G. Simultaneous manipulation of polarization relaxation and conductivity toward self-repairing reduced graphene oxide based ternary hybrids for efficient electromagnetic wave absorption. *J. Colloid. Interface. Sci.* **2023**, *630*, 453-64. DOI PubMed
8. Li, Z.; Zhu, H.; Rao, L.; et al. Wrinkle structure regulating electromagnetic parameters in constructed core-shell ZnFe₂O₄@PPy microspheres as absorption materials. *Small* **2024**, *20*, e2308581. DOI
9. Ma, L.; Wei, L.; Hamidinejad, M.; Park, C. B. Layered polymer composite foams for broadband ultra-low reflectance EMI shielding: a computationally guided fabrication approach. *Mater. Horiz.* **2023**, *10*, 4423-37. DOI
10. Xu, M.; Wei, L.; Ma, L.; et al. Microcellular foamed polyamide 6/carbon nanotube composites with superior electromagnetic wave absorption. *J. Mater. Sci. Technol.* **2022**, *117*, 215-24. DOI
11. Guo, J.; Li, X.; Chen, Z.; et al. Magnetic NiFe₂O₄/polypyrrole nanocomposites with enhanced electromagnetic wave absorption. *J. Mater. Sci. Technol.* **2022**, *108*, 64-72. DOI
12. Sun, Y.; Han, X.; Guo, P.; et al. Slippery graphene-bridging liquid metal layered heterostructure nanocomposite for stable high-

- performance electromagnetic interference shielding. *ACS. Nano.* **2023**, *17*, 12616-28. DOI
13. Wu, J.; Wang, K.; Ye, S.; et al. One-pot synthesis of conductive metal-organic framework@polypyrrole hybrids with enhanced electromagnetic wave absorption performance. *Small. Struct.* **2024**, *5*, 2400205. DOI
 14. He, W.; Zheng, J.; Dong, W.; et al. Efficient electromagnetic wave absorption and Joule heating via ultra-light carbon composite aerogels derived from bimetal-organic frameworks. *Chem. Eng. J.* **2023**, *459*, 141677. DOI
 15. Guo, Z.; Ren, P.; Yang, F.; et al. Robust multifunctional composite films with alternating multilayered architecture for highly efficient electromagnetic interference shielding, Joule heating and infrared stealth. *Compos. Part. B. Eng.* **2023**, *263*, 110863. DOI
 16. Liu, S.; Qin, S.; He, M.; et al. Construction and application of flexible electromagnetic interference shielding films with multifunctionality. *Compos. Commun.* **2024**, *50*, 102011. DOI
 17. Zhao, T.; Jia, Z.; Liu, J.; Zhang, Y.; Wu, G.; Yin, P. Multiphase interfacial regulation based on hierarchical porous molybdenum selenide to build anticorrosive and multiband tailorable absorbers. *Nanomicro. Lett.* **2023**, *16*, 6. DOI PubMed PMC
 18. Xu, P.; Huang, B.; Tang, R.; Wang, Z.; Tu, J.; Ding, Y. Improved mechanical and EMI shielding properties of PLA/PCL composites by controlling distribution of PIL-modified CNTs. *Adv. Compos. Hybrid. Mater.* **2022**, *5*, 991-1002. DOI
 19. Zhang, B.; Wu, C.; Ye, K.; Sun, C.; Wang, Z. Dual-induced SiC/SME multifunction composite for high - Efficiency broadband electromagnetic wave absorption. *Carbon* **2023**, *213*, 118253. DOI
 20. Wang, C.; Liu, Y.; Jia, Z.; Zhao, W.; Wu, G. Multicomponent nanoparticles synergistic one-dimensional nanofibers as heterostructure absorbers for tunable and efficient microwave absorption. *Nanomicro. Lett.* **2022**, *15*, 13. DOI PubMed PMC
 21. Cheng, Z.; Zhou, J.; Liu, Y.; et al. 3D printed composites based on the magnetoelectric coupling of Fe/FeCo@C with multiple heterogeneous interfaces for enhanced microwave absorption. *Chem. Eng. J.* **2024**, *480*, 148188. DOI
 22. Zhou, B.; Song, J.; Wang, B.; Feng, Y.; Liu, C.; Shen, C. Robust double-layered ANF/MXene-PEDOT:PSS Janus films with excellent multi-source driven heating and electromagnetic interference shielding properties. *Nano. Res.* **2022**, *15*, 9520-30. DOI
 23. Yang, R.; Zhang, D.; Gao, H.; Wang, Y.; Li, N.; Zhang, H. Size-progressively-reduced FeCoNi@C nanoparticles spatially confined within polypyrrole-derived hollow carbon nanoboxes against electromagnetic contamination. *Chem. Eng. J.* **2024**, *495*, 153114. DOI
 24. Duan, Y.; Xu, P.; Liu, T.; et al. Design of PDMS/SiO₂/MXene composites with "Floatable Interlayer" structure for the electromagnetic shielding behavior improvement. *Chem. Eng. J.* **2023**, *461*, 141853. DOI
 25. Yuan, L.; Zhao, W.; Miao, Y.; et al. Constructing core-shell carbon fiber/polypyrrole/CoFe₂O₄ nanocomposite with optimized conductive loss and polarization loss toward efficient electromagnetic absorption. *Adv. Compos. Hybrid. Mater.* **2024**, *7*, 864. DOI
 26. Sun, M.; Wang, D.; Xiong, Z.; et al. Multi-dimensional Ni@C-CoNi composites with strong magnetic interaction toward superior microwave absorption. *J. Mater. Sci. Technol.* **2022**, *130*, 176-83. DOI
 27. Dong, C.; Li, D.; Wang, H.; et al. CoSe₂@polythiophene core-shell composites with enhanced interfacial polarization for high-performance broadband electromagnetic absorption. *Carbon* **2023**, *215*, 118459. DOI
 28. Sharma, G. K.; James, N. R. Aligned, carbon nanofibers containing barium titanate and their polydimethylsiloxane composites for electromagnetic interference shielding. *Carbon* **2024**, *220*, 118846. DOI
 29. Xu, C.; Ma, L.; Li, H.; et al. Biomass derived PANI/BPC composite with enhanced polarization loss for efficient electromagnetic wave absorption. *Mater. Res. Bull.* **2024**, *176*, 112805. DOI
 30. Cao, K.; Yang, X.; Zhang, Y.; et al. Preparation of magnetic three-dimensional porous Co-rGO aerogel for enhanced microwave absorption. *Carbon* **2023**, *208*, 111-22. DOI
 31. Yu, M.; Huang, Y.; Liu, X.; et al. Synthetic strategy of biomimetic sea urchin-like Co-NC@PANI modified MXene-based magnetic aerogels with enhanced electromagnetic wave absorption properties. *Nano. Res.* **2024**, *17*, 2025-37. DOI
 32. Liu, S.; Qin, S.; Jiang, Y.; Song, P.; Wang, H. Lightweight high-performance carbon-polymer nanocomposites for electromagnetic interference shielding. *Compos. Part. A. Appl. Sci. Manuf.* **2021**, *145*, 106376. DOI
 33. Liu, X.; Huang, Y.; Zhao, X.; Yan, J.; Zong, M. Flexible N-doped carbon fibers decorated with Cu/Cu₂O particles for excellent electromagnetic wave absorption. *J. Colloid. Interface. Sci.* **2022**, *616*, 347-59. DOI
 34. Sharma, S.; Pratap, S. B.; Hur, S. H.; Choi, W. M.; Chung, J. S. Facile fabrication of stacked rGO/MoS₂ reinforced polyurethane composite foam for effective electromagnetic interference shielding. *Compos. Part. A. Appl. Sci. Manuf.* **2023**, *166*, 107366. DOI
 35. Bai, Y.; Yang, H.; He, L.; Ge, C.; Zhai, R.; Zhang, X. Construction of core-shell BN-OH@Fe₃O₄@PAN nanocomposite with ultra-wide microwave absorption and efficiency thermal management. *J. Alloys. Compd.* **2023**, *936*, 168174. DOI
 36. Wang, C.; Wang, Y.; Jiang, H.; et al. Three-dimensional bamboo-like amorphous N/S co-doped carbon nanotubes encapsulated with Cu nanoparticles/carbon fiber heterostructures for boosting electromagnetic wave absorbing properties. *Ceram. Int.* **2023**, *49*, 2792-805. DOI
 37. Rao, L.; Li, Z.; Qian, Y.; et al. Heterointerface engineering in porous microspheres for magnetic-dielectric balance to boost electromagnetic wave absorption. *Chem. Eng. J.* **2024**, *488*, 150955. DOI
 38. Tan, D.; Wang, Q.; Li, M.; et al. Magnetic media synergistic carbon fiber@Ni/NiO composites for high-efficiency electromagnetic wave absorption. *Chem. Eng. J.* **2024**, *492*, 152245. DOI
 39. Feng, S.; Wang, H.; Ma, J.; et al. Fabrication of hollow Ni/NiO/C/MnO₂@polypyrrole core-shell structures for high-performance electromagnetic wave absorption. *Compos. Part. B. Eng.* **2024**, *275*, 111344. DOI
 40. Dhugga, L. K.; Baskey, H. B.; Gaur, K. K.; Singh, D. P. Absorption dominant electromagnetic interference shielding in the novel polypyrrole-CaCu₃Ti₄O₁₂-CoFe₂O₄ nanocomposites. *Compos. Sci. Technol.* **2023**, *240*, 110067. DOI
 41. Patle, V. K.; Mehta, Y.; Dwivedi, N.; Mondal, D.; Srivastava, A.; Kumar, R. Thermal insulating and fire-retardant lightweight

- carbon-slag composite foams towards absorption dominated electromagnetic interference shielding. *Sustain. Mater. Technol.* **2022**, *33*, e00453. DOI
42. Ma, Z.; Deng, Z.; Zhou, X.; et al. Multifunctional and magnetic MXene composite aerogels for electromagnetic interference shielding with low reflectivity. *Carbon* **2023**, *213*, 118260. DOI
 43. Zhang, H.; Cao, F.; Xu, H.; et al. Plasma-enhanced interfacial engineering of FeSiAl@PUA@SiO₂ hybrid for efficient microwave absorption and anti-corrosion. *Nano. Res.* **2023**, *16*, 645-53. DOI
 44. Dong, F.; Dai, B.; Zhang, H.; et al. Fabrication of hierarchical reduced graphene oxide decorated with core-shell Fe₃O₄@polypyrrole heterostructures for excellent electromagnetic wave absorption. *J. Colloid. Interface. Sci.* **2023**, *649*, 943-54. DOI
 45. Wu, N.; Zhao, B.; Lian, Y.; et al. Metal organic frameworks derived Ni_xSe_y@NC hollow microspheres with modifiable composition and broadband microwave attenuation. *Carbon* **2024**, *226*, 119215. DOI
 46. Huyan, W.; Yao, J.; Tao, J.; et al. MXene@C heterogeneous nanocomposites with the 2D-0D structure for ultra-light and broadband electromagnetic wave absorption. *Carbon* **2022**, *197*, 444-54. DOI
 47. Tian, X.; Xu, X.; Bo, G.; Su, X.; Yan, J.; Yan, Y. A 3D flower-like Fe₃O₄@PPy composite with core-shell heterostructure as a lightweight and efficient microwave absorbent. *J. Alloys. Compd.* **2022**, *923*, 166416. DOI
 48. Yang, D.; Tao, J.; Yang, Y.; et al. Effect interfacial size and multiple interface on electromagnetic shielding of silicon rubber/carbon nanotube composites with mixing segregated particles. *Compos. Struct.* **2022**, *292*, 115668. DOI
 49. Liu, S.; He, M.; Zhang, D.; et al. New construction strategies of carbon-based composites for flexible electromagnetic interference shielding films. *Polym. Compos.* **2024**, *45*, 5804-26. DOI
 50. Li, Z.; Xu, C.; Zheng, J.; et al. Robust and flexible composite aerogel films with porous multilayered structures toward broadband electromagnetic wave absorption. *J. Mater. Chem. C.* **2024**, *12*, 3632-43. DOI
 51. Liu, Y.; Wang, F.; Wang, Y.; et al. A combined engineering of hollow and core-shell structures for C@MoS₂ microcapsules toward high-efficiency electromagnetic absorption. *Compos. Part. B. Eng.* **2024**, *273*, 111244. DOI
 52. Zeng, Y.; Long, L.; Yu, J.; Li, Y.; Li, Y.; Zhou, W. High-efficiency electromagnetic wave absorption of lightweight Nb₂O₅/CNTs/polyimide with excellent thermal insulation and compression resistance integration. *Compos. Sci. Technol.* **2024**, *250*, 110531. DOI
 53. Shao, S.; Guo, C.; Wang, H.; et al. Multifunctional graphene/Ti₃C₂T MXene aerogel inlaid with Ni@TiO₂ core-shell microspheres for high-efficiency electromagnetic wave absorption and thermal insulation. *Chem. Eng. J.* **2024**, *488*, 150918. DOI
 54. Qin, L.; Liu, S.; Qin, S.; Liao, L.; He, M.; Yu, J. MOF derived porous Ni/Co@C nanocomposite as electromagnetic wave absorber with optimized impedance matching. *Compos. Commun.* **2022**, *33*, 101196. DOI
 55. Yu, M.; Huang, Y.; Liu, X.; Zhao, X.; Fan, W.; She, K. In situ modification of MXene nanosheets with polyaniline nanorods for lightweight and broadband electromagnetic wave absorption. *Carbon* **2023**, *208*, 311-21. DOI
 56. Qin, L.; Liu, S.; Yang, J.; He, M.; Yu, J. Carbon nanotube modified hierarchical NiCo/porous nanocomposites with enhanced electromagnetic wave absorption. *J. Alloys. Compd.* **2023**, *966*, 171599. DOI
 57. Pan, F.; Cai, L.; Shi, Y.; et al. Heterointerface engineering of β-chitin/carbon nano-onions/Ni-P composites with boosted maxwell-wagner-sillars effect for highly efficient electromagnetic wave response and thermal management. *Nanomicro. Lett.* **2022**, *14*, 85. DOI PubMed PMC
 58. Zhang, Y.; Zhang, L.; Tang, L.; Du, R.; Zhang, B. S-NiSe/HG nanocomposites with balanced dielectric loss encapsulated in room-temperature self-healing polyurethane for microwave absorption and corrosion protection. *ACS. Nano.* **2024**, *18*, 8411-22. DOI
 59. Dou, Y.; Zhang, X.; Zhao, X.; et al. N, O-doped walnut-like porous carbon composite microspheres loaded with Fe/Co nanoparticles for adjustable electromagnetic wave absorption. *Small* **2024**, *20*, e2308585. DOI
 60. Liu, S.; Yang, J.; Fan, Q.; He, L.; Qin, S.; He, M. Surface modification of basalt fibers with improved reactivity, thermal stability, and tensile strength. *Fibers. Polym.* **2024**, *25*, 3403-13. DOI
 61. Liu, S.; Luo, D.; He, M.; Qin, S. In situ crosslinking of silica aerogel with reactive carbon fiber for high mechanical property, thermal insulation and superhydrophobicity. *Micropor. Mesopor. Mat.* **2024**, *377*, 113203. DOI
 62. Wei, J.; Shao, G.; Huang, X. Freeze-cast Ni-MOF nanobelts/chitosan-derived magnetic carbon aerogels for broadband electromagnetic wave absorption. *ACS. Appl. Mater. Interfaces.* **2024**, *16*, 20969-79. DOI
 63. Xu, P.; He, H.; Fang, J.; et al. Design and fabrication of a hollow nanobowl-like heterostructured PPy@Co/CoFe₂O₄@HNBC composite as a remarkable electromagnetic wave absorber. *J. Alloys. Compd.* **2022**, *926*, 166749. DOI
 64. Gao, Y.; Wu, Q.; Pan, L.; et al. Ordered heterostructured aerogel for multi-spectra stealth in microwave, infrared and visible light bands. *Chem. Eng. J.* **2024**, *484*, 149422. DOI
 65. Zheng, S.; Wang, Y.; Wang, X.; Lu, H. Research progress on high-performance electromagnetic interference shielding materials with well-organized multilayered structures. *Mater. Today. Phys.* **2024**, *40*, 101330. DOI
 66. Huang, P.; Wang, Y.; El-Shorbagy, M.; Akhtar, M. N.; Hoi, H. T. Optical and electromagnetic absorption features of hierarchical pampon and cauliflower-like magneto/dielectric composite based absorber for C and X bands application. *Ceram. Int.* **2022**, *48*, 16280-9. DOI
 67. Deng, Y.; Ren, B.; Jia, Y.; Wang, Q.; Li, H. Layered composites made of polymer derived SiOC/ZrB₂ reinforced by ZrO₂/SiO₂ fibers with simultaneous microwave absorption and thermal insulation. *J. Mater. Sci. Technol.* **2024**, *196*, 50-9. DOI
 68. Tang, Y.; Wang, Y.; Huang, M.; Wang, M. Effect of interfacial morphology on electromagnetic shielding performance of poly (l-lactide)/polydimethylsiloxane/multi-walled carbon nanotube composites with honeycomb like conductive networks. *Polym. Compos.* **2024**, *45*, 2253-67. DOI

69. Ma, R.; Yi, S.; Li, J.; et al. Highly efficient electromagnetic interference shielding and superior mechanical performance of carbon nanotube/polydimethylsiloxane composite with interface-reinforced segregated structure. *Compos. Sci. Technol.* **2023**, *232*, 109874. DOI
70. Ma, Z.; Jiang, R.; Jing, J.; et al. Lightweight dual-functional segregated nanocomposite foams for integrated infrared stealth and absorption-dominant electromagnetic interference shielding. *Nanomicro. Lett.* **2024**, *16*, 223. DOI PubMed PMC
71. Tan, Y.; Xue, Y.; Li, K.; et al. PVDF/MWCNTs/RGO@Fe₃O₄/AgNWs composite film with a bilayer structure for high EMI shielding and electrical conductivity. *Polym. Compos.* **2023**, DOI
72. Liu, T.; Zhang, N.; Zhang, K.; Wang, Y.; Qi, Y.; Zong, M. Multi-components matching manipulation of MXene/PPy@β₂-SiW₁₁Co/Fe₃O₄ nanocomposites for enhancing electromagnetic wave absorption performance. *Compos. Part. A. Appl. Sci. Manuf.* **2022**, *159*, 107020. DOI
73. Zhang, Y.; Feng, Y.; Li, J.; et al. Multi-interfacial bridging engineering of flexible MXene film for efficient electromagnetic shielding and energy conversion. *J. Colloid. Interface. Sci.* **2024**, *665*, 733-41. DOI
74. Tao, W.; Ma, M.; Liao, X.; et al. Cellulose nanofiber/MXene/mesoporous carbon hollow spheres composite films with porous structure for decreased reflected electromagnetic interference shielding. *Compos. Commun.* **2023**, *41*, 101647. DOI
75. Tang, P.; Li, M.; Du, J.; et al. Construction of Fe₃O₄/PANI composites with hollow 0D/1D structures for efficient microwave absorption. *Appl. Surf. Sci.* **2024**, *649*, 159183. DOI
76. Wang, X.; Li, C.; Geng, H.; et al. Tunable dielectric properties and electromagnetic wave absorbing performance of MoS₂/Fe₃O₄/PANI composite. *Colloid. Surfaces. A.* **2022**, *637*, 128285. DOI
77. Xiao, C.; Liu, S.; Gong, Y.; Liu, Y.; He, M.; Yu, J. Reinforcement of polyamide 6 with carbon fiber surface modified by a polar cross-linked network interfacial phase. *J. Mater. Res. Technol.* **2023**, *24*, 362-75. DOI
78. Liu, X.; Sun, H.; Yan, W.; Yang, S.; Jiang, X. Fabrication and microwave absorption properties of FeSiAl@PANI composites. *ACS. Appl. Electron. Mater.* **2024**, *6*, 394-405. DOI
79. Hu, K.; Wan, X.; Lai, S.; et al. Preparation of polyaniline/sludge fly ash with improved electromagnetic microwave absorption performance. *Mater. Lett.* **2022**, *316*, 132061. DOI
80. Tho, P.; Tran, N.; Tuan, N.; et al. Detailed microwave loss mechanisms for nanocomposites of La-doped BaFe₁₂O₁₉ and polyaniline. *Ceram. Int.* **2023**, *49*, 23669-79. DOI
81. Liu, Z.; Zhao, X.; Jiang, X.; Yan, X.; Yu, L. Carbon microspheres/carbon sheets as efficient electromagnetic wave absorbers. *Micropor. Mesopor. Mat.* **2024**, *372*, 113090. DOI
82. Wu, W.; Yuan, S.; Zhang, W.; et al. Preparation and performance of a bamboo-based electromagnetic wave absorber by interfacial polymerization of graphene oxide/polyaniline. *Arab. J. Chem.* **2024**, *17*, 105651. DOI
83. Liu, X.; Huang, Y.; Zhao, X.; Han, X.; Jia, Y.; Zong, M. Core-shell N-doped carbon nanofibers@poly(3,4-ethylenedioxythiophene): Flexible composite fibers for enhanced electromagnetic wave absorption. *Compos. Part. A. Appl. Sci. Manuf.* **2022**, *163*, 107227. DOI
84. Çelebi, N.; Soysal, F.; Salimi, K. Well-defined core/shell pDA@Ni-MOF heterostructures with photostable polydopamine as electron-transfer-template for efficient photoelectrochemical H₂ evolution. *Int. J. Hydrogen. Energy.* **2022**, *47*, 13828-37. DOI
85. Li, X.; Luo, J.; Wang, Q.; Wu, Y.; Dai, Z.; Xie, Y. Polydopamine-derived nitrogen-doped carbon coupled with MoSe₂ nanosheets composites toward high-efficiency electromagnetic wave absorption. *Carbon* **2024**, *225*, 119119. DOI
86. Jiang, W.; Jiang, B.; Yang, J.; Wang, M. Q.; Li, Y. High electrical conductivity and π-π stacking interface design for tunable electromagnetic wave absorption composite foams. *J. Mater. Chem. C.* **2022**, *10*, 15458-65. DOI
87. Li, Y.; Li, X.; Li, Q.; Zhao, Y.; Wang, J. Low-energy-consumption fabrication of porous TPU/graphene composites for high-performance microwave absorption and the influence of Fe₃O₄ incorporation. *J. Alloys. Compd.* **2022**, *909*, 164627. DOI
88. Li, Y.; Zhang, D.; Zhou, B.; et al. Synergistically enhancing electromagnetic interference shielding performance and thermal conductivity of polyvinylidene fluoride-based lamellar film with MXene and graphene. *Compos. Part. A. Appl. Sci. Manuf.* **2022**, *157*, 106945. DOI
89. Xu, Y.; Tan, Y.; Xue, Y.; et al. A novel PVA/MWCNTs hydrogel with high toughness and electromagnetic shielding properties. *Polym. Eng. Sci.* **2023**, *63*, 3555-64. DOI
90. Yang, R.; Zhou, Y.; Ren, Y.; et al. Promising PVDF-CNT-Graphene-NiCo chains composite films with excellent electromagnetic interference shielding performance. *J. Alloys. Compd.* **2022**, *908*, 164538. DOI
91. Yang, R.; Tan, Y.; Zhou, T.; et al. A PVDF/MWCNTs/GO@MWCNTs/AgNWs bilayer structured composite film with ultra-high EMI shielding and conductivity performance. *Polym. Compos.* **2024**, *45*, 11044-61. DOI
92. Liu, Y.; Zhan, Y.; He, M.; et al. Amino-functionalized carbon fiber/polyamide 6 composites with enhanced interfacial and mechanical properties. *J. Mater. Res. Technol.* **2022**, *20*, 3229-40. DOI
93. Feng, Y.; Liao, H.; Wang, J. Multifunctional melamine-based multilayer foam with heterogeneous alternating structure towards electromagnetic interference shielding. *Colloid. Surface. A.* **2023**, *674*, 131953. DOI
94. Du, B.; Zhang, G.; Huan, X.; et al. Electrostatically self-assembled Fe₃O₄@SiO₂/MXene 3D interlayered structure improves Ku-band microwave absorption efficiency of epoxy-based nanocomposites. *Compos. Part. A. Appl. Sci. Manuf.* **2024**, *177*, 107956. DOI
95. Qian, Y.; Luo, Y.; Haruna, A. Y.; et al. Multifunctional epoxy-based electronic packaging material MDCF@LDH/EP for electromagnetic wave absorption, thermal management, and flame retardancy. *Small* **2022**, *18*, e2204303. DOI
96. Luo, J.; Yang, X.; Xue, Y.; et al. High-performance, multifunctional, and designable carbon fiber felt skeleton epoxy resin

- composites EP/CF-(CNT/AgBNs)_x for thermal conductivity and electromagnetic interference shielding. *Small* **2024**, *20*, e2306828. DOI
97. Anju; Masař, M.; Machovský, M.; et al. Optimization of CoFe₂O₄ nanoparticles and graphite fillers to endow thermoplastic polyurethane nanocomposites with superior electromagnetic interference shielding performance. *Nanoscale. Adv.* **2024**, *6*, 2149-65. DOI PubMed PMC
98. Sun, Z.; Shen, J.; Chen, W.; et al. High-performance polyurethane composite elastomers with coral reef-like hierarchical heterostructures for electromagnetic wave absorption and flexible sensing. *Mater. Today. Chem.* **2024**, *35*, 101840. DOI
99. Xiao, W.; Zhang, L.; Zhang, S.; Yan, J.; Zhang, G.; Gao, J. Electrically conductive and magnetic nanofiber composites with an asymmetric structure for efficient electromagnetic interference shielding. *Colloids. Surf. A. Physicochem. Eng. Asp.* **2023**, *675*, 132063. DOI
100. Ye, L.; Liu, L.; Yin, G.; et al. Highly conductive, hydrophobic, and acid/alkali-resistant MXene@PVDF hollow core-shell fibers for efficient electromagnetic interference shielding and Joule heating. *Mater. Today. Phys.* **2023**, *35*, 101100. DOI
101. Suresh, S.; Krishnan, V. G.; Dasgupta, D.; Surendran, K. P.; Gowd, E. B. Directional-freezing-enabled MXene orientation toward anisotropic PVDF/MXene aerogels: orientation-dependent properties of hybrid aerogels. *ACS. Appl. Mater. Interfaces.* **2023**, *15*, 49567-82. DOI
102. Lee, S.; Nguyen, N. K.; Kim, M.; Park, P.; Nah, J. Conductivity-controlled polyvinylidene fluoride nanofiber stack for absorption-dominant electromagnetic interference shielding materials. *ACS. Appl. Mater. Interfaces.* **2023**, *15*, 33180-9. DOI
103. Guo, Z.; Ren, P.; Yang, F.; et al. MOF-derived Co/C and MXene co-decorated cellulose-derived hybrid carbon aerogel with a multi-interface architecture toward absorption-dominated ultra-efficient electromagnetic interference shielding. *ACS. Appl. Mater. Interfaces.* **2023**, *15*, 7308-18. DOI
104. Du, Y.; Xu, J.; Fang, J.; et al. Ultralight, highly compressible, thermally stable MXene/aramid nanofiber anisotropic aerogels for electromagnetic interference shielding. *J. Mater. Chem. A.* **2022**, *10*, 6690-700. DOI
105. Lu, X.; Zhu, D.; Li, X.; Wang, Y. Architectural design and interfacial engineering of CNTs@ZnIn₂S₄ heterostructure/cellulose aerogel for efficient electromagnetic wave absorption. *Carbon* **2022**, *197*, 209-17. DOI
106. Lu, Z.; Wang, Y.; Di, X.; Wang, N.; Cheng, R.; Yang, L. Heterostructure design of carbon fiber@graphene@layered double hydroxides synergistic microstructure for lightweight and flexible microwave absorption. *Carbon* **2022**, *197*, 466-75. DOI
107. Sun, M.; Guo, Z.; Zhang, W.; et al. A strategy to fabricate hierarchical microporous architecture of polyimide nanofibrous aerogels with efficient electromagnetic wave absorption and thermal insulation. *Compos. Part. A. Appl. Sci. Manuf.* **2024**, *177*, 107940. DOI
108. Geng, T.; Yu, G.; Shao, G.; Huang, X. Enhanced electromagnetic wave absorption properties of ZIF-67 modified polymer-derived SiCN ceramics by in situ construction of multiple heterointerfaces. *Rare. Met.* **2023**, *42*, 1635-44. DOI
109. Xu, R.; Zhou, J.; Huang, W.; et al. Polymer-derived silicon oxycarbonitride bowls with hollow structures and hetero-nanodomains for electromagnetic wave absorption. *J. Mater. Chem. C.* **2024**, *12*, 4640-7. DOI